



# Multiorgan-on-a-chip: an advanced platform for disease modeling, drug toxicity assessment, and therapeutic screening

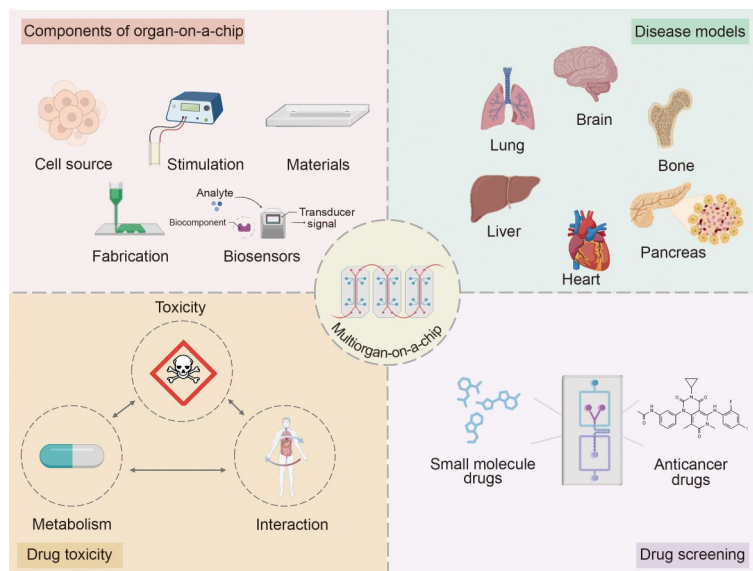
Li Qiao<sup>1</sup> · Shiqi Chang<sup>1</sup> · Lin Zou<sup>1</sup> · Feng Zhang<sup>2</sup> · Chang Cui<sup>2</sup> · Ningping Huang<sup>1</sup>

Received: 19 February 2025 / Accepted: 26 May 2025 / Published online: 14 November 2025  
© Zhejiang University Press 2025

## Abstract

Multiorgan-on-a-chip (MOoC) systems are advanced microfluidic devices that integrate multiple organ models into a single modular unit, each composed of cells derived from various tissues or organs. These systems enable interorgan communication and accurately replicate physiological conditions, providing a more physiologically relevant modeling framework for constructing disease models and predicting drug efficacy and toxicity. MOoC systems also provide significant advantages in terms of flexibility, cost-effectiveness, and reproducibility, making them valuable tools for drug development and toxicity assessment. In this review, we first provide an overview of the MOoC technology, covering cell sources, stimulations, materials and fabrication techniques, and biosensors. We then examine the application of MOoC systems in disease modeling, focusing on cancer metastasis, metabolic disorders, and cardiovascular disease. We next discuss the use of MOoC systems in drug toxicity evaluation and drug screening, emphasizing their role in providing comprehensive assessments of drug effects. Finally, we address the challenges it faces and the future perspectives of the MOoC technology.

## Graphical abstract



**Keywords** Multiorgan-on-a-chip · Disease modeling · Drug toxicity · Drug screening

✉ Ningping Huang  
nphuang@seu.edu.cn

<sup>1</sup> State Key Laboratory of Digital Medical Engineering, School of Biological Science and Medical Engineering, Southeast University, Nanjing 210096, China

<sup>2</sup> Department of Cardiology, The First Affiliated Hospital with Nanjing Medical University, Nanjing 210029, China

## 1 Introduction

Biomedical research has traditionally relied on two-dimensional (2D) cell cultures and animal models for disease modeling and drug screening [1, 2], which have yielded valuable insights into disease mechanisms and played a vital role in therapeutic development. However, 2D cell cultures, which grow as monolayers in Petri dishes, lack both the structural complexity and dynamic conditions of *in vivo* tissues. These limitations restrict their ability to replicate human pathophysiology, drug response, and toxin interactions [3]. Furthermore, primary cells have limited passage capabilities, whereas immortalized cell lines often accumulate mutations during prolonged culturing, thereby compromising their reliability. The static nature of these cultures further exacerbates these issues, as they lack essential features such as vascular flow and interstitial dynamics, which are critical for mimicking the physiological microenvironment. Although animal models remain the gold standard for preclinical drug validation and represent a more holistic system to investigate drug metabolism and effects [4], they have significant limitations. In addition, physiological and genetic differences between animals and humans often result in inconsistencies in drug efficacy and safety, thereby reducing their predictive accuracy for human outcomes.

The emergence of the organ-on-a-chip (OoC) technology has revolutionized disease modeling and drug screening, representing a promising alternative to traditional cell and animal models [5]. These microengineered platforms replicate the structural and functional complexity of human organs by integrating living cells and biomaterials within a microfluidic device [6]. This setup allows precise control over the cellular microenvironment, enabling the study of human physiology and the side effects of drugs in a more realistic context. The OoC technology provides several key advantages, including a more reliable and predictive model for investigating drug safety and efficacy, supporting high-throughput screening, reducing costs, and accelerating the drug discovery process [7]. Over the past decade, OoC systems have rapidly evolved to target various organs, such as the heart [8], lung [9], kidney [10], liver [11], and gut [12]. As single OoC systems have matured further, researchers have focused more attention on multiorgan-on-a-chip (MOoC) or body-on-a-chip [13]. MOoC systems integrate multiple organ models such as the heart, liver, lung, and kidney within a single microfluidic device, allowing simulation of organ–organ interactions and systemic responses *in vitro*. This innovative approach addresses several limitations inherent in conventional models, thus providing a more holistic view of disease progression and drug effects.

In this review, we aim to present a comprehensive overview of the current applications of the MOoC technology, which include cell sources, stimulations, materials, fabrication

techniques, and integrated biosensors. We will also explore their applications in disease modeling, drug toxicity assessment, and drug screening. Finally, we conclude by addressing the current challenges and discussing potential future developments in this field (Fig. 1).

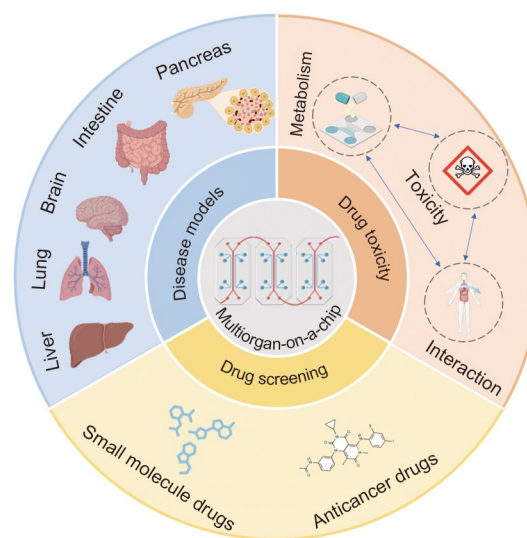


**Fig. 1** Schematic of the MOoC systems discussed in this review, including their applications in disease modeling, drug toxicity testing, and drug screening. Created using BioRender (<https://app.biorender.com>)

## 2 Overview of MOoC

MOoC is an innovative biomedical engineering approach in which cells obtained from multiple human organs or tissues are cultured on a microchip to replicate critical functions of human physiological systems. A typical MOoC device includes miniature chambers, fluidic channels, and sensors that accurately mimic the physiological conditions of specific organs [14]. The selection of appropriate cell types is critical to the success of the system, as different cell types must be carefully selected based on the specific experimental objectives. Various stimuli, such as electrical signals [15], mechanical stretching [16, 17], fluid flow [18], and chemical signals [19], are applied to the microsystem to improve tissue maturation and functional performance *in vitro*. Integrated biosensors enable real-time monitoring of cellular responses, including metabolic activity, cell viability, and cell death, thereby enabling the evaluation of drug effects. The modular design of MOoC systems allows the customization of materials and fabrication methods, providing researchers with the flexibility to address diverse experimental requirements. These features position MOoC as a versatile tool for exploring interorgan communication, drug metabolism pathways, and systemic toxicity mechanisms (Fig. 2).

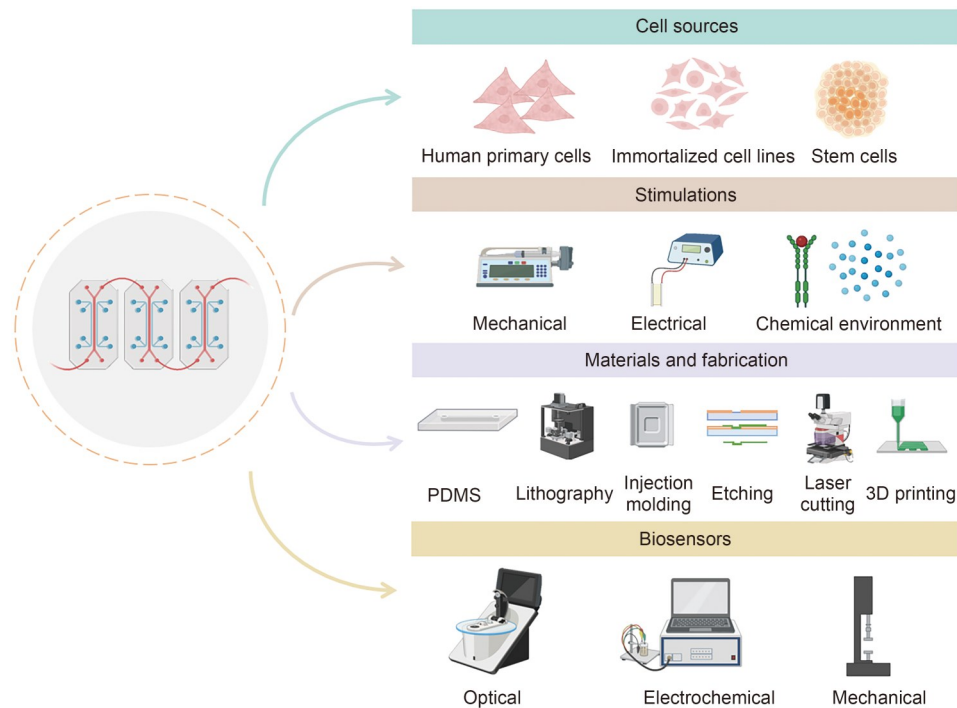


**Fig. 2** The MOoC platform integrates essential elements including cell sources, stimulation systems, materials, fabrication methods, and biosensors. Created using BioRender (<https://app.biorender.com>)

## 2.1 Cell sources

Cell sources for OoC systems can be classified into the following three categories based on cost, availability, and tissue functionality: human primary cells, immortalized cell lines, and stem cells [20]. Each of these cell types has its own set of advantages and disadvantages.

Human primary cells are extracted from living organs, typically obtained from biopsy material, and have been successfully used in liver [21], lung [22], kidney proximal tubule [23], and neurovascular-on-a-chip systems [24]. They retain the donor's genotype, rendering them suitable for personalized drug screening applications. However, they may harm the donors, and their limited proliferative capacity and phenotypic changes after being cultured for a few passages result in a short lifespan and restrict applicability in OoC studies. Immortalized cell lines can be easily cultured and are readily available for multiple passages without significant changes in phenotype, thereby allowing for the generation of reproducible outcomes [25]. Nevertheless, they cannot completely replicate the intricate organ functions observed *in vivo* and may not accurately represent the heterogeneous cellular response found in living organisms due to their genetic and phenotypic uniformity [26]. Stem cells include embryonic stem cells, induced pluripotent stem cells (iPSCs), and adult stem cells, among which iPSCs have gained increasing popularity for drug testing and disease modeling [27]. iPSCs are generated by reprogramming

adult cells, such as skin fibroblasts [28], adipose stromal cells [29], peripheral blood samples [30], and urine samples [31]. They can be subsequently differentiated into any desired cell type using small molecules or commercial kits. The advantages of iPSCs include noninvasive access to patients' cells, convenience for investigating drug efficacy at a personalized level, and the avoidance of ethical issues. Nonetheless, the application of iPSC-derived cells may be limited by their immature phenotypes and may require additional stimuli to achieve full functionality. Furthermore, the production of iPSCs can be expensive and technically challenging, which may limit their widespread application in OoC systems.

Over the past century, cell culture has relied on static nutrient environments that facilitated proliferation but often resulted in reduced tissue functionality. Recent advances using three-dimensional (3D) extracellular matrix (ECM) hydrogels within microphysiological systems have provided innovative platforms for investigating human biology and pathology. These models successfully emulate native tissue architecture, cell–cell communication, and essential physiological processes. Although static models demonstrate utility in replicating certain tissue-level functions, their inability to incorporate dynamic physiological elements, such as multi-tissue integration, circulatory networks, biomechanical forces, and systemic immune interactions, limits their accuracy in modeling compound biodistribution and clearance processes. Such limitations compromise their ability to

accurately simulate drug distribution patterns, metabolic clearance, and potential adverse effects across different tissues. Microfluidic organ-chip platforms address these gaps by engineering controlled microenvironments that recapitulate organ-level transport barriers, fluid shear stresses, metabolite exchange rates, and oxygen gradients, thereby significantly improving the physiological relevance of pharmacokinetic–pharmacodynamic (PK/PD) evaluations [32].

## 2.2 Stimulations

Tissues cultured in OoC systems often require physical or chemical stimulation to promote tissue maturation and functionality. In vivo, cells are exposed to a combination of biomechanical and biochemical stimuli, such as mechanical stimuli, electrical stimulation, and chemical environment, which interact to modulate cellular responses [33]. To better mimic physiological conditions, OoC systems incorporate various mechanical stimuli, which can be categorized into the following three types: shear flow, compression, and stretch/strain [34]. Shear flow can be further classified into laminar flow, pulsatile flow, and interstitial flow. These mechanical forces play a significant role in regulating cell behaviors such as proliferation, migration, phenotype maintenance, and differentiation.

Laminar flow has been widely utilized in OoC systems to explore the effects of fluid forces on angiogenesis, the process of forming new blood vessels, and drug toxicity in liver-on-a-chip models [35–37]. Remarkably, laminar shear stress also plays a vital role in the development of intestinal villi morphology in gut-on-a-chip systems, demonstrating its importance in tissue morphogenesis [38]. Pulsatile flow is commonly applied in blood-vessel-on-chip systems to replicate the natural pulsation of blood flow within the human circulatory system [39]. The effect of interstitial flow on cell motility has also been extensively investigated, with microfluidic systems emerging as a promising platform for exploring this phenomenon. For instance, interstitial flow has been used in lung-on-a-chip [40] and intestine-on-a-chip [41] models to mimic biological processes and improve cell differentiation. Moreover, compression stresses are particularly relevant for modeling mechanically active tissues such as the skin [42] and cardiac tissue [43], whereas stretch/strain conditions are essential for simulating lung alveoli and intestinal peristalsis in respective chip models [44, 45].

Electrical stimulation is a pivotal element within OoC systems [46], which is recognized for its ability to improve tissue functionality and expedite the maturation of cardiomyocytes (CMs). In these systems, controlled electrical signals are generated through electrodes and subsequently applied to cells within the device. Platinum and gold electrodes are used to deliver electrical signals, which not only

stimulate iPSC-derived CMs (iPSC-CMs) but also record electrophysiological signals in real time [47].

Beyond mechanical and electrical stimulation, the chemical environment plays a crucial role in the generation and maintenance of physiologically accurate OoC systems [48]. Growth factors and cytokines are essential for replicating the tissue microenvironment. To achieve precise spatiotemporal control over chemical factors within the microenvironment, researchers can use microfluidic devices that incorporate pressure regulation at the inlet [49]. For instance, *Xenopus laevis* (frog) animal cap explants represent a highly integrated multicellular system that allows for long-term and high-speed experiments, facilitated by the control of inlet pressure. This approach has been confirmed to be highly effective for investigating tissue responses to the steroid hormone dexamethasone (DEX) [50].

## 2.3 Materials and fabrication of OoC devices

### 2.3.1 Materials of OoC devices

Polydimethylsiloxane (PDMS) is a crucial material extensively utilized in OoC research [51]. It is commonly used as the primary structure or as a porous membrane in most devices [52]. PDMS has numerous unique advantages for OoC applications, including long-term biocompatibility for cultured cells, ease of fabrication, optical transparency for observing and evaluating tissues, high elasticity, low toxicity, excellent oxygen permeability, and cost-effectiveness [53]. Nevertheless, PDMS does have several drawbacks, which have prompted researchers to explore alternative materials in the realm of OoC. A well-known limitation of PDMS is its hydrophobicity and capacity to absorb lipophilic compounds [54]. This characteristic can interfere with drug testing outcomes, resulting in inaccuracies in the evaluation of drug toxicity and efficacy. To improve PDMS adhesion, researchers have investigated surface or membrane coating with ECM proteins, such as collagen, gelatin [55], fibronectin, and hydrogels [56]. These coatings generate a natural environment for cell adhesion and the formation of functional tissue structures. Although PDMS is widely used in the OoC field, it may not be the ideal material for fabricating OoCs dedicated to drug testing, personalized medicine, and absorption, distribution, metabolism, and excretion (ADME) modeling. A review by Campbell et al. highlighted various alternative materials to PDMS for OoC applications, each with distinct advantages [57]. For instance, elastomers, composed of intertwined polymer chains, provide flexibility and stretchability and also resist the absorption of small hydrophobic molecules, thus addressing a key limitation of PDMS, and are often used in heart-on-a-chip systems [58]. Thermoplastic polymers are another cost-effective alternative with reduced risk of monomer leaching,

excellent biocompatibility, and robust mechanical properties, although they lack the flexibility of PDMS [57]. Poly-methyl methacrylate (PMMA) stands out for its optical clarity and mechanical strength. In addition, epoxy is valued for its durability and resistance to harsh chemicals [59]. These materials demonstrate a diverse range of properties, catering to the specific requirements of OoC fabrication.

### 2.3.2 Fabrication methods of OoC devices

The transition from laboratory prototypes to clinically viable OoC devices necessitates careful consideration of fabrication scalability. Although rapid prototyping methods (e.g., soft lithography and 3D printing) dominate academic research due to their design flexibility, they face inherent limitations in production throughput and reproducibility. In contrast, wafer-level photolithography and industrial injection molding demonstrate proven scalability for high-volume manufacturing, although with higher initial tooling costs. There are several approaches for fabricating OoC devices, including lithography [60], injection molding [61], etching, laser cutting processes [62], and 3D printing [63].

(i) Lithography technology, a cornerstone of semiconductor manufacturing, is extensively used in OoC fabrication and can be divided into two major types, namely, photolithography and soft lithography. In ultraviolet (UV) lithography processes, light exposure transfers intricate 3D patterns from a photomask to a photoresist-coated silicon substrate [64]. SU-8 is a commonly used photoresist type in microfabrication. In photolithography, a photosensitive layer undergoes a chemical transformation when exposed to light, resulting in the hardening of specific areas but leaving others soft. Subsequently, the unexposed regions are baked and washed away in a chemical bath, and the hardened parts remain adhered to the silicon wafer. Subsequent etching steps transfer these patterns into the underlying substrate [65]. Although photolithography achieves precise and high-resolution microfabrication, its implementation requires significant infrastructure investment, including cleanroom facilities and specialized equipment [66].

Soft lithography extends the capabilities of conventional photolithography by replicating microstructures/nanostructures on elastomeric materials. The process begins with the fabrication of a master mold using high-resolution techniques such as electron-beam lithography and two-photon polymerization, which determine the final pattern resolution (as fine as 30 nm) and feature size range (10–100 nm) [67]. This mold subsequently transfers the patterns to PDMS through molding, providing cost-effective prototyping solutions, although with limited production scalability.

(ii) Injection molding is a high-throughput manufacturing process used for the mass production of parts through the injection of molten material into a mold [68]. This process

typically utilizes a thermoplastic or thermosetting polymer that is heated to a viscous state and then forcibly injected into a mold cavity under high pressure. The molding process involves the following four sequential steps: clamping, injection, cooling, and ejection. The mold is first tightly clamped, and then the molten polymer is forced through a plunger into the cavity. Phase-change cooling is accelerated by integrated water channels. After solidification, the mold opens and the ejector pins. The mold is then closed, and the process is repeated. Compared with PDMS-based fabrication methods, injection molding demonstrates superior performance in terms of cell loading efficiency and ECM-mimetic capability and also maintains production scalability.

(iii) The etching technique represents a fundamental subtractive process in microfabrication, with two principal variants, namely, wet etching (chemical solution-based) and dry etching (plasma-based) [69]. In a standard wet etching protocol, researchers first deposit an etch-resistant mask (typically a photoresist or silicon nitride) patterned by lithography to expose targeted substrate regions. The exposed area is then selectively removed by chemical immersion. Wet etching can generate an isotropic profile. Dry etching methods address the isotropic limitations of wet etching by producing anisotropic profiles, although they require more sophisticated equipment. Despite being indispensable for prototyping microfluidic platforms, their scalability for true industrial-scale production remains challenged due to throughput limitations, material selectivity constraints, and environmental concerns [70].

(iv) Laser cutting process is a popular method for fabricating microfluidic channels and is compatible with a range of materials such as plastic and glass, thereby enabling the creation of different patterns with various depths and widths on the substrate using computer-aided design. This technology provides the advantages of being a relatively rapid and straightforward process that does not require a cleanroom environment for fabrication [71]. Nevertheless, laser cutting has the drawback of requiring expensive equipment, limiting its use for large-scale production.

(v) The 3D printing technology has found applications across various industries, including healthcare, aerospace, automotive, and consumer products. The landscape of 3D printing has expanded to encompass a range of different technologies, such as fused deposition modeling, selective laser sintering, and digital light processing [72]. 3D printing enables the accurate and customizable fabrication of intricate structures, making it possible to generate highly accurate models of human organs and tissues. Using 3D printing for the development of OoC devices allows researchers to more faithfully replicate the complex environments of human organs and tissues, resulting in more accurate drug testing and disease modeling. Nonetheless, although 3D printing excels in prototyping and small-batch fabrication,

its scalability to industrial-scale production remains a challenge due to printing speed, cost, and standardization. Various techniques are available for fabricating OoCs, with the choice of the fabrication method and materials dependent on the specific objectives of the study.

## 2.4 Biosensors

The integration of biosensors into OoC technology has led to a remarkable transformation in drug development and disease modeling. Biosensor devices are designed to promptly detect and quantify biological or chemical substances in real time, making them highly valuable in various OoC models, including those focusing on metabolism, barrier function, muscle tissue, and neuronal activity [73]. Biosensors can be broadly categorized into the following three types based on their transduction mechanisms: optical, electrochemical/electrical, and mechanical [74, 75]. These sensors enable the precise monitoring of cellular responses, improving the accuracy and relevance of OoC systems for biomedical research.

Optical biosensors have been integral to MOoC systems due to their high sensitivity, specificity, and dynamic sensing capabilities [76]. These sensors utilize advanced photonic technologies to detect changes in optical absorption, luminescence intensity, refractive index, and incident/reflected light angles [77]. Their wavelength-specific colorimetric responses enable the quantitative evaluation of various physiological parameters, including metabolic activity, cellular pathology, tissue viability, proliferation, and intercellular communication [78]. A key benefit of optical sensing lies in its oxygen-independent operation, which eliminates redox reactions. Oxygen detection typically uses fluorescent dyes or phosphorescent nanoparticles, where the emission characteristics (intensity/lifetime) undergo reversible modulation through oxygen-dependent collisional quenching [79]. Such systems enable spatial mapping by fluorescence lifetime imaging microscopy. For monitoring pH, phenol red serves as an effective optical indicator in the culture medium. This water-soluble compound exhibits pH-dependent absorption spectra, transitioning from red to yellow across physiological ranges. Khalid et al. successfully implemented this system in lung-on-a-chip systems to quantify cell death through the release of acidic byproducts [80]. Similarly, Shaegh et al. developed optical sensor modules for the dynamic measurement of pH and dissolved oxygen levels in the culture medium in microfluidic bioreactors and OoC devices [81]. Optical sensors provide remarkable advantages for real-time monitoring applications. For instance, Shang et al. developed an anisotropic inverse opal substrate with periodic elliptical macropores and hydrogel filling, enabling self-driven actuation and self-reported feedback [82]. In this system, CMs were cultured on the

substrate, resulting in highly aligned cell organization with autonomic beating ability. The dynamic contraction and relaxation of the CMs induced synchronous deformation in the inverse opal structure. These mechanical forces were optically detectable through structural color variations or spectral shifts in the engineered cardiac tissue model, thus providing a noninvasive method for the quantification of cellular forces. This system holds promise for applications in cell behavior monitoring and drug screening. By combining optogenetic control mechanisms with visually responsive bioactuators, this approach paves the way for integrated real-time detection and self-regulating feedback systems.

Electrochemical biosensors commonly depend on the binding of an analyte to its immobilized bioreceptor on the working electrode, with the resulting signal being comparable to that of an uncoated reference electrode [83, 84]. For instance, enzymatic electrochemical biosensors such as glucose and lactate sensors operate by utilizing enzyme-catalyzed reactions to detect analyte concentrations [85]. The microcurrents produced during these reactions are subsequently detected and used for quantifying analyte concentrations [86]. Biosensors can also be seamlessly integrated into OoC systems to measure transendothelial/epithelial electrical resistance (TEER). TEER is often used to evaluate the barrier function of models, such as the gut [87], lung [88], and blood–brain barrier (BBB) [89]. For instance, Henry et al. demonstrated an advanced two-channel organ chip featuring embedded electrodes for continuous, noninvasive TEER monitoring of cultured cell monolayers [88]. This approach enables real-time evaluation of barrier function dynamics across multiple tissue types.

Mechanical sensors play a vital role in evaluating cellular forces and biomechanical properties, enabling the study of physiological processes such as lung motion, vascular shear stress, intestinal peristalsis, and skin tension. These systems can replicate key aspects of the tissue microenvironment, including cyclic strain and fluid-induced shear forces. For instance, Shin et al. engineered a gut-on-a-chip microdevice and a Transwell-insertable hybrid chip seeded with Caco-2 cells or intestinal organoids. By modulating basolateral fluid flow, they achieved functional regeneration of the intestinal microarchitecture within five days, demonstrating how mechanical stimuli influence tissue development [90]. Furthermore, mechanical sensing facilitates biomechanical analysis, cardiac physiological research, and drug screening. For instance, Lind et al. developed an innovative cardiac microphysiological device using multimaterial 3D printing, incorporating soft strain gauges into microstructures that promote the self-organization of physiologically relevant cardiac tissues. These embedded sensors enabled noninvasive monitoring of contractile stresses, allowing for long-term observation of drug responses and tissue maturation over four weeks [91]. Similarly, Qu et al. designed a

microelectromechanical system-based cardiac microarray using human iPSC-CMs (hiPSC-CMs), where tissue contraction was quantified via pillar deflection. This platform detected the pharmacological effects of isoprenaline and amiodarone, revealing a direct correlation between changes in drug-induced contractility and pillar displacement [92].

This incorporation of biosensors into OoC devices demonstrates significant potential for advancing drug development. It allows for real-time monitoring, improving the precision of drug efficacy and safety evaluations, and contributes to a deeper understanding of disease mechanisms.

Furthermore, we introduced the key components of OoC technology that have enabled the development of various single-organ models, such as the heart [93], liver [94], kidney [95], intestine [96], lung [97], and skin [98] systems. These models are commonly used for disease modeling, drug toxicity assessment, and drug screening. Nevertheless, as the human body operates as an interconnected system where organs interact with each other, single-organ models fail to completely simulate the complex *in vivo* microenvironment. This limitation has driven the development of MOoC systems designed to address these drawbacks by replicating interorgan interactions. MOoC systems achieve this by integrating microfluidic channels that interconnect different organ models or by designing multiple organ systems on a single chip [99]. Common MOoC configurations include organ pairings that replicate critical physiological interactions, such as heart–liver, heart–tumor, liver–kidney, liver–intestine, and lung–liver in two-organ-on-a-chip

systems. More complex setups include three-organ-on-a-chip systems such as cardiac–liver–lung and cardiac–liver–skeletal; four-organ-on-a-chip systems such as heart–liver–skeletal muscle–neuronal, intestine–liver–skin–kidney, and heart–liver–bone–skin; and even larger configurations such as seven-organ-on-a-chip systems (brain–heart–liver–lung–pancreas–gut–endometrium) or ten-organ-on-a-chip systems (liver–pancreas–gut–lung–heart–muscle–brain–endometrium–skin–kidney). The most complex MOoC systems can integrate up to 13 organs, including fat, kidney, heart, adrenal glands, liver, spleen, pancreas, bone marrow, brain, muscle, skin, gastrointestinal (GI) tract, and lungs, providing more comprehensive simulations of human physiological processes. In subsequent sections, we explore the applications of MOoC systems in disease modeling, drug toxicity evaluation, and drug screening.

### 3 MOoC for disease modeling

In recent years, the MOoC technology has gained significant attention as a powerful tool for disease modeling. It connects single OoC systems or integrates multiple organs onto a single chip platform [100]. MOoC devices provide a more physiologically relevant environment for investigating complex diseases. This section explores the application of MOoC systems in disease modeling, focusing on the construction of diverse models, the relevant organs involved, and the recreation of their microenvironments (Table 1). This section also highlights case studies on specific diseases,

**Table 1** Summary of disease models developed on MOoC platforms: disease types, distinctive capabilities, and biological insights

| Disease model       | Disease                                  | Description  | Finding   | Reference   |
|---------------------|--|--|---|---|
| Cancer              | Oral squamous cell carcinoma (OSCC)      | Self-aligning TetrIs-Like (TILE) modular microfluidic platform | Facilitating the integration of existing organs-on-a-chip   | [101]   |
|                     | Lung cancer                              | An upstream “lung organ” and three downstream “distant organs” | Recapitulating the tumor microenvironment and lung cancer metastasis  | [102]   |
| Metabolic disorders | Nonalcoholic fatty liver disease (NAFLD) | Gut–liver interconnect via circulation channels                | Facilitating the construction of disease models, such as inflammatory bowel disease (IBD) and liver disease models  | [103]   |
|                     | Diabetes                                 | Human pancreas-on-a-chip                                       | Integration with Raman microspectroscopy for real-time insulin monitoring   | [104]   |
|                     | Type 2 diabetes mellitus (T2DM)          | Coculture of primary human liver spheroids and islets          | A modular system where different tissues are actuated simultaneously, followed by controlled integration of tissue-specific signals   | [105]   |
|                     | Jaundice                                 | Blood vessel–skin–liver–lung organ-on-a-chip                   | Constructing a jaundice disease model and potential treatment   | [106]   |
|                     | Cardiovascular diseases                  | Myocardial infarction (MI)                                     | Capillary blood flow–endothelial cell–myocardial tissue structure   | Mimicking a physiological fluidic microenvironment and hypoperfusion/hypoxia conditions during MI |
|                     | MI                                       | Border-zone-on-a-chip  | Cardiac tissue cultured on dual serpentine microchannels with differential gas perfusion to form an oxygen gradient; cardiac functions and transcription analyses being performed | [108]   |

including cancer, metabolic disorders, and cardiovascular diseases.

### 3.1 Cancer

Cancer is a primary cause of death worldwide, with approximately 10 million fatalities reported in 2022 by the International Agency for Research on Cancer (IARC) [109]. Early diagnosis and effective treatment are crucial in clinical oncology, driving researchers to focus on identifying early biomarkers for both detection and therapeutic intervention. Nevertheless, replicating the complexity of the tumor microenvironment that includes both biochemical and biophysical factors presents significant challenges when using traditional *in vivo* and *in vitro* models [110]. The MOoC technology represents a promising alternative by integrating multiple organ systems and providing a more accurate simulation of the tumor environment than conventional approaches. Human physiology and pathophysiology often involve multiple tissues, especially in complex processes such as cancer metastasis, a process involving circulating tumor cells that colonize different organs. Predicting affected organs and designing novel treatment strategies for metastasis requires integrating multiple organs, a challenge addressed by the MOoC technology. Ong et al. developed a TetrIs-Like (TILE) modular microfluidic platform featuring a “stick-n-play” design to explore metastatic oral squamous cell carcinoma (OSCC) [101]. By incorporating patient-derived primary/metastatic tumors with liver, endothelial modules, and tumor modules, the system used residence time scaling to mimic organ-specific pharmacokinetics. Remarkably, cyclophosphamide bioactivation by HepaRG-derived hepatocytes improved tumor cell killing in both primary and metastatic modules, effectively reversing the “apparent” resistance of metastatic OSCC tumors. This finding not only validates the ability of the platform to model organ-specific drug metabolism but also emphasizes its potential for predicting the efficacy of personalized therapeutics (Fig. 3a).

Further advancing metastasis research, Xu et al. constructed an MOoC system to mimic lung cancer formation and metastasis processes with an *in vivo*-like environment [102]. The system was constructed using three PDMS layers and two thin microporous PDMS membranes. It featured an upstream “lung organ” and three downstream “distant organs” comprising astrocytes, osteoblasts, and hepatocytes that simulate lung cancer metastasis to the brain, bone, and liver. The design recapitulated the key hallmarks of metastasis-epithelial-mesenchymal transition (EMT) and CXCR4/RANKL/AFP overexpression in brain, bone, and liver modules, consistent with *in vivo* observations in nude mice. The capacity of this system to capture both early invasion (via EMT) and organotropic colonization (through

receptor–ligand axis activation) establishes a paradigm for investigating metastatic organotropism. Miller et al. developed a microphysiological system modeling human colorectal cancer (CRC) metastasis from the colon to liver [111]. This two-chamber colon–liver device interconnected both compartments to simulate metastatic progression. The system maintained high cell viability and also cultured normal/cancerous colon organoids with liver sinusoidal endothelial components. Researchers investigated the metastatic capacity of single cancer cells and the penetration of cancer cell clusters through layers of the healthy colon. The two methods yielded consistent experimental outcomes. The adjustable parameters of the platform (e.g., glucose concentration and hypoxia) enabled the investigation of clinically relevant questions (Fig. 3b). Lee et al. constructed a bone-on-a-chip model for osteoporosis-related bone metastasis [112]. The device cocultured three bone cell types (osteocyte, osteoblast, and osteoclast) in different ratios. Triple-negative breast cancer cells (MDA-MB-231) were injected into the vascular channel. The authors demonstrated increased cancer cell invasion under osteoporotic conditions compared with that under other conditions. This effect may be attributed to the increased number of osteoclasts in the osteoporotic tissue, which is probably mediated by increased vascular permeability that facilitates transendothelial migration. These advanced models bridge the gap between 2D drug screening and animal studies by enabling the simultaneous analysis of primary tumor behavior and distant organ responses, providing critical insights for the development of antimetastasis drugs.

### 3.2 Metabolic disorders

Metabolic disorders, including obesity, coronary artery disease, cardiovascular disease, nonalcoholic fatty liver disease (NAFLD), and type 2 diabetes mellitus (T2DM), are complex pathological conditions shaped by genetic predisposition and environmental effects [113]. Among them, NAFLD is the most prevalent chronic liver disorder that is clinically defined by abnormal hepatic fat deposition [114]. This condition exhibits progressive pathogenesis, evolving from steatosis to nonalcoholic steatohepatitis (NASH) and potentially advancing to irreversible liver fibrosis and cirrhosis. Although contemporary research implicates hepatic inflammation and steatosis as characteristic of disease progression, their precise relationship remains unclear [115]. Recent advances in OoC technology now enable the precise dissection of these interactions through human-relevant systems.

Yang et al. developed an integrated-gut-liver-on-a-chip (iGLC) platform to investigate the progression of NAFLD under controlled metabolic stress [103]. This innovative system featured closed-loop circulation between intestinal and

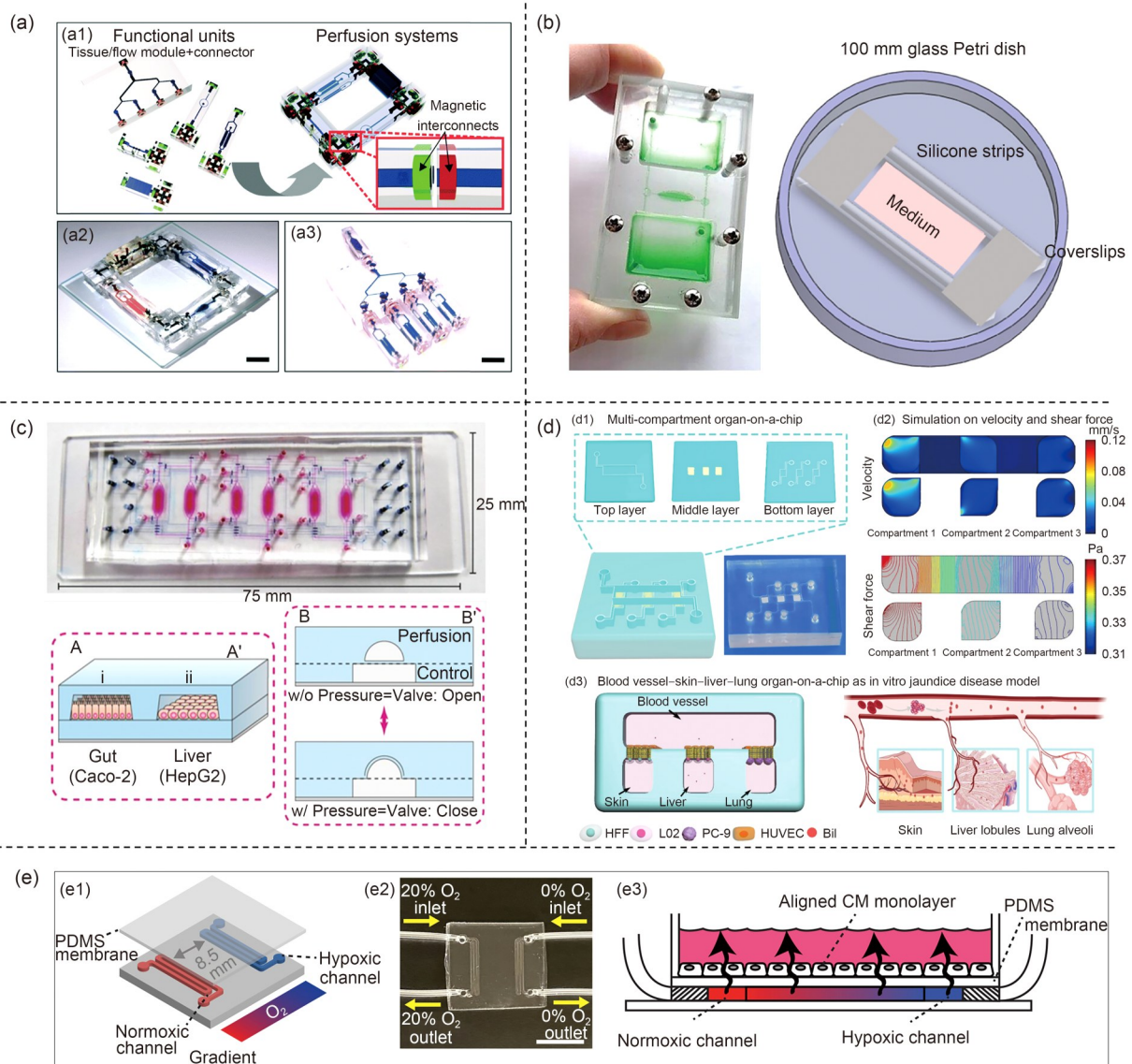


**Fig. 3** MOOC systems for disease modeling. (a) Fabrication and characterization of the back-compatible TILE system. The image illustrates the assembly of the TILE modules into functional perfusion systems, which include a recirculating perfusion system and a one-pass parallel perfusion system. Reproduced from [101], Copyright 2019, with permission from The Royal Society of Chemistry. (b) A visible gut–liver unidirectional device with cell chambers and channels, which can fit into a 100-mm glass Petri dish. Reproduced from [111], Copyright 2024, with permission from Wiley Periodicals LLC. (c) A photograph of an iGLC platform shows its perfusion (pink) and control (blue) layers. The lower panel provides a cross-sectional view of the cell culture chambers, which were seeded with Caco-2 gut cells and HepG2 liver cells, along with the integrated microvalves in both open and closed states. Reproduced from [103], Copyright 2023, with permission from the authors, licensed under CC BY 4.0. (d) The fabrication of MC-OoC and the construction of blood vessel–skin–liver–lung organ-on-a-chip as an in vitro jaundice disease model. Reproduced from [106], Copyright 2021, with permission from Donghua University, Shanghai, China. (e) Oxygen gradient conditions were established by gas flow through serpentine microchannel networks, with cardiac cells cultured on a fibronectin membrane. Reproduced from [108], Copyright 2022, with permission from the authors, licensed under CC BY-NC

hepatic compartments, exposing the cocultures to free fatty acids (FFAs) and revealing tissue-specific responses; the intestinal cells upregulated retinol metabolism genes, and the hepatocytes exhibited lipid accumulation and endoplasmic reticulum stress markers. Remarkably, this dual-tissue interaction amplified the toxicity of FFAs compared with monocultures, accurately recapitulating the clinical progression

of NAFLD from localized lipid overload to systemic metabolic dysfunction. The platform’s ability to synchronously track phenotypic changes positions it as a critical tool for identifying early biomarkers of NASH transition (Fig. 3c).

Diabetes, a complex multisystem metabolic disorder, involves dysregulation across multiple organ systems [116].

Although current management typically involves lifestyle changes or medication such as metformin, its underlying mechanisms remain poorly understood. To address specific discrepancies in diabetes research, Zbinden et al. developed a human pancreas-on-a-chip platform featuring self-organizing  $\beta$ -cell pseudoislets [104]. This PDMS-based system combined vasculature-mimetic perfusion with noninvasive Raman spectroscopy, enabling real-time monitoring of insulin secretion dynamics. This innovation circumvents the invasive sampling limitations of animal models and also preserves the functionality of human islets. A major risk factor for T2DM is the abnormal glucose homeostasis between the pancreas and liver. Although existing models have explored the interaction between islets and the liver, only a few have integrated primary human liver and islet cultures. To fill this gap, Shafagh et al. developed a microphysiological multi-tissue OoC that cocultured 3D primary human liver spheroids and human pancreatic islets [105]. This device was assembled from components fabricated using off-stoichiometric thiol-ene-epoxy (OSTE+), PMMA, and PDMS. The microfluidic features were etched into a PMMA block using CO<sub>2</sub> laser technology, and an aluminum mold was used to shape the middle layer. The components were securely clamped together with PMMA, ensuring effective sealing of the chambers and channels. The device incorporated a central chamber connected to satellite chambers through microfluidic channels. This design enables the simultaneous actuation of different tissues and controlled integration of tissue-specific signals to realize reciprocal communication on a physiological timescale. In the liver-on-a-chip, the liver also exhibits characteristics of a physiological hepatic insulin response due to the interaction between the two organs. By integrating transcriptomic signatures with functional outputs, this model bridges the gap between genetic susceptibility studies and clinical phenotypes, providing a roadmap for screening personalized anti-diabetic drugs.

Lei et al. developed a nanofiber-enabled multicompartiment organ-on-a-chip (MC-OoC) platform to model jaundice [106]. This MC-OoC system was used to establish a multiorgan model, specifically a blood vessel–skin–liver–lung configuration that demonstrated the differential cytotoxicity of bilirubin (Fig. 3d). Jaundice develops from a disorder in bilirubin metabolism in the liver, resulting in elevated bilirubin levels in the bloodstream. This excess bilirubin binds readily to elastin in the skin, causing the characteristic yellow discoloration and also potentially damaging pulmonary epithelial cells. To explore a potential treatment, researchers applied blue light therapy at various intensities (405 nm), a standard clinical approach for reducing bilirubin levels in patients with jaundice [117]. Results demonstrated a gradual improvement in cell viability, confirming that blue light can effectively mitigate bilirubin-induced

cytotoxicity. This study showed that the *in vitro* jaundice model successfully mimicked the disease process, as evidenced by the decline in cell viability upon bilirubin exposure and its recovery after blue light treatment. This approach provides a paradigm for investigating metabolic disorders involving distant organ crosstalks, such as hyperbilirubinemia-induced multiorgan failure.

### 3.3 Cardiovascular diseases

MOoC platforms have been instrumental in investigating various heart diseases, particularly myocardial infarction (MI), a leading cause of mortality worldwide [118]. MI occurs when a coronary artery becomes occluded, resulting in oxygen deprivation in the downstream cardiac tissue. This oxygen deficit triggers sarcolemmal disruption, mitochondrial dysfunction, and widespread cell death and necrosis, which can begin as early as 20 min after the onset of ischemia [119]. Considering the complexity of these processes, replicating them *in vitro* requires highly specialized systems that can simulate the dynamic blood flow and cellular microenvironments found in the heart. To address this challenge, Ren et al. developed an MI model that exemplifies this progress by stimulating both the hemodynamic and biochemical aspects of ischemia [107]. Through precise dual-channel perfusion control, the system replicated physiological blood flow and hypoperfusion, exhibiting cell loss and caspase-3 activation patterns reflecting the progression of clinical ischemia. Importantly, the integration of carbonyl cyanide *p*-trifluoromethoxyphenylhydrazone (FCCP)-induced chemical hypoxia revealed dose-dependent mitochondrial depolarization, a mechanism vital to reperfusion injury. This dual physical–chemical approach accurately mimics the pathological conditions of MI, addressing a key limitation of static *in vitro* models. Furthermore, Rexius-Hall et al. developed a microphysiological system to controllably expose engineered cardiac tissue to the interface between hypoxic and normoxic tissues. This system was characterized by an oxygen gradient, which was used to examine the impact of oxygen gradients on the function of cardiac tissue [108]. The chip contained two serpentine microchannels, and controlled gas perfusion was used to mimic the oxygen gradient. Neonatal rat ventricular myocytes were seeded on a membrane that was microcontact-printed with lines of fibronectin. After three days, the cells formed an anisotropic myocardial tissue. By determining the effects of the gradient on electromechanical function and transcription, it was found that the gradient delayed calcium release and reduced systolic pressures, along with activation of inflammatory cascades and increase of MI marker levels (Fig. 3e). These results indicate that the oxygen gradient at the boundary between normoxia and hypoxia induces unique regulatory processes, which may trigger ventricular

arrhythmias and potentially cause sudden cardiac death. The clinical relevance of the platform is emphasized by its ability to dissect therapeutic targets. Specifically, by isolating endothelial–myocardial interactions under flow, it enables high-throughput testing of cardioprotective agents that target mitochondrial integrity or apoptosis pathways. Such systems are poised to accelerate drug discovery by providing human-relevant readouts of ischemic damage and also circumventing species-specific limitations of animal models.

MOoC systems have revolutionized disease modeling by providing platforms that closely replicate human physiology and the intricate interactions between multiple organs. These advanced systems enable researchers to simulate complex disease states and explore organ-to-organ communication, making them especially valuable for understanding diseases such as cancer, metabolic disorders, and cardiovascular disease. Prominent case studies emphasize the versatility of MOoC systems in tailoring models for specific disease conditions, facilitating deeper insights into disease mechanisms, drug responses, and potential therapeutic interventions. As technological advancements continue, MOoC platforms are poised to play an increasingly vital role in bridging the gap between traditional *in vitro* studies and clinical practice, ultimately improving drug development processes and the practice of personalized medicine.

## 4 MOoC used for drug toxicity

Drug toxicity plays a vital role in the progression from synthesis to the preclinical stage. Numerous drugs have encountered regulatory scrutiny or been discontinued by manufacturers after extensive preclinical and clinical trials due to unanticipated toxicity in humans. The human body comprises interconnected tissues that operate within a complex interactive network, where the activity in one tissue can impact others downstream [120]. MOoC systems simulate these interconnections by linking various organs, allowing for the simulation of drug processing as it occurs *in vivo*. This section explores drug toxicity in MOoC systems, emphasizing essential elements such as drug metabolism, toxicity assessment, and interactions between organs.

### 4.1 Drug metabolism evaluations in MOoC systems

Drug metabolism is a key factor in determining the efficacy and safety of a drug [121]. MOoC systems simulate *in vivo* drug metabolism by integrating critical organ models, such as the liver, intestine, and kidney.

The liver is the largest internal organ in the human body and plays a vital role in the metabolism of drugs and the regulation of the half-life of drugs [122]. These functions can

exert side effects due to exposure to drugs or their metabolites. Although the liver possesses remarkable regenerative capacities, it can sustain significant damage from chronic liver diseases such as viral or alcoholic hepatitis, potentially resulting in permanent loss of function [123]. Drug-induced liver injury is a major concern during drug development, and regulatory agencies such as the United States Food and Drug Administration (FDA) often issue warnings or restrictions on drug use when liver toxicity concerns arise [124]. Animal models cannot completely replicate the *in vivo* architecture of the human liver. In recent years, advancements in microfluidic and microfabrication technologies have emerged as vital tools for investigating drug toxicity. Microfluidic OoC systems provide several advantages, including precise control over physiologically relevant parameters and the ability to replicate the characteristic features of the liver on a microscale. For instance, Delalat et al. developed a liver-on-a-chip system that cultured primary hepatocytes in 3D heparin-coated microtrenches for four weeks to evaluate chronic hepatotoxicity [125]. This platform has been confirmed effective in evaluating liver toxicity. The liver is essential for metabolizing xenobiotic compounds, facilitating their elimination from the body. Therefore, liver metabolism can produce metabolites that are either more toxic or more effective than the original drug. Cyclophosphamide is typically considered noncardiotoxic; however, it can produce cardiotoxic metabolites during hepatic transformation. Oleaga et al. developed a multiorgan microfluidic device that integrates heart cells derived from iPSCs and primary hepatocytes [126]. The platform, constructed from PDMS using laser cutting technology, features five interconnected chambers. This system was used to explore cyclophosphamide-induced alterations in cardiac electrical activity, in both the presence and absence of hepatocytes. Their study demonstrated that cardiotoxicity was detected only when hepatocytes were included, thus emphasizing the role of hepatic metabolites. Remarkably, replacing the medium on Day 5 or 6 to eliminate hepatic metabolites allowed CMs to recover within 48 h. This cost-effective, user-friendly heart–liver system allows for the coculture of human CMs and hepatocytes in a serum-free defined medium under gravitational flow conditions, making it ideal for investigating drug metabolism related to cardiotoxicity (Fig. 4a). Furthermore, Yin et al. designed a liver-heart-organoids-on-a-chip system derived from hiPSCs, which features four layers as follows: the upper microwell chamber for liver organoid cultures and the bottom chamber with a micropillar array to form embryoid bodies with consistent morphology [127]. When liver and heart organoids were cocultured on the chip, the liver organoids synthesized albumin and urea, whereas the cardiac organoids exhibited functional beating. Clomipramine, an FDA-approved tricyclic antidepressant, causes significant cell death in cardiac

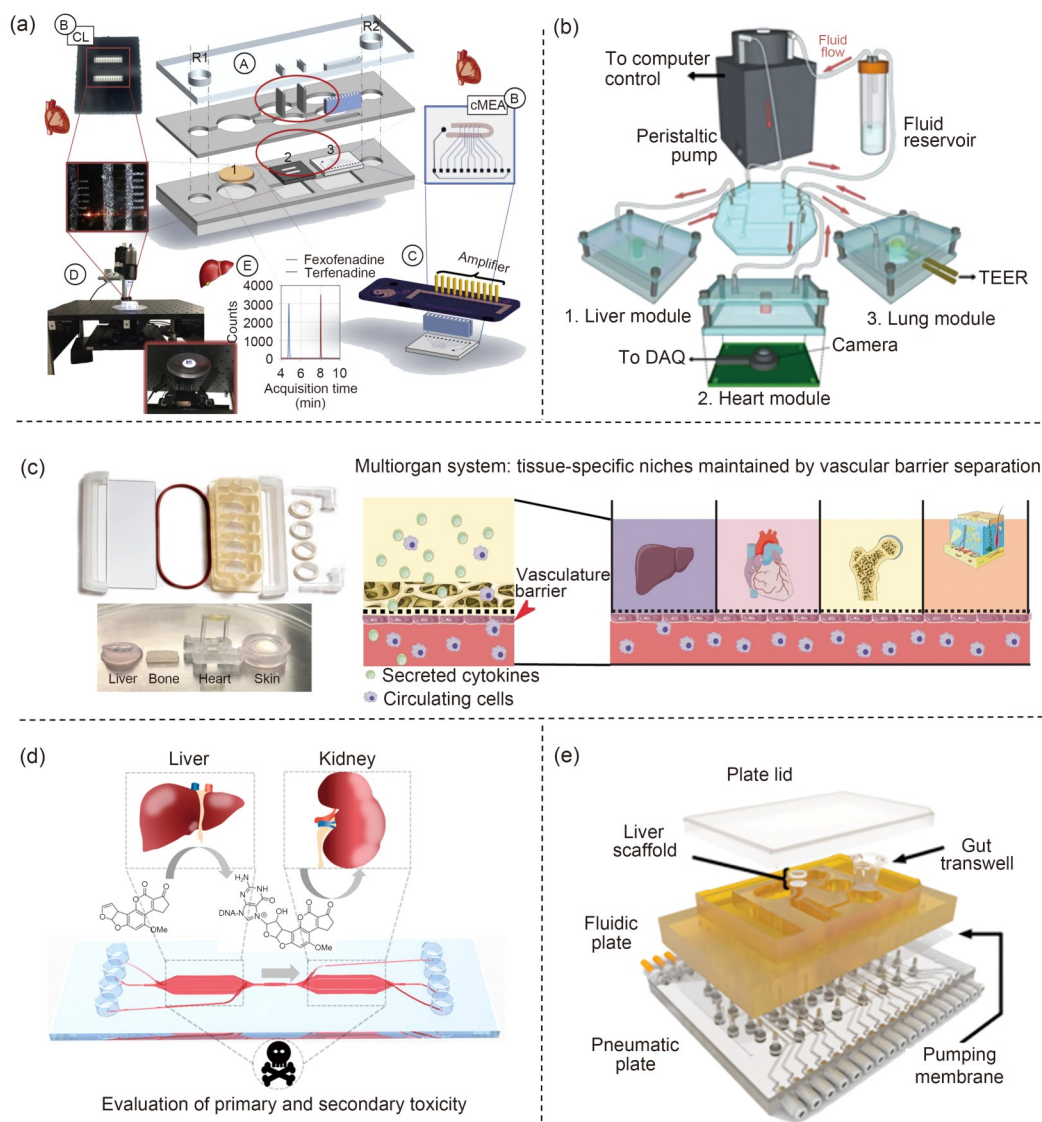


**Fig. 4** Drug metabolism and toxicity in MOoC systems. (a) A pumpless microfluidic system facilitates heart–liver coculture, which enables evaluating the metabolism and toxicity of cyclophosphamide and terfenadine. Reproduced from [126], Copyright 2018, with permission from Elsevier. (b) A heart–liver–lung organ-on-a-chip using bioprinting technology to evaluate the toxicity of bleomycin. Reproduced from [128], Copyright 2017, with permission from the authors, licensed under CC BY. (c) A liver–heart–bone–skin tissue platform interconnected via recirculating vascular flow allows for “plug-and-play.” Reproduced from [129], Copyright 2022, with permission from the authors, under exclusive licence to Springer Nature Limited. (d) A liver–kidney-on-a-chip model investigated both the primary and secondary toxic effects of AFB1 and B $\alpha$ P on liver and kidney tissues. Reproduced from [133], Copyright 2017, with permission from the American Chemical Society. (e) Detailed overview of the design and operation of a gut–liver organ-on-a-chip platform. Reproduced from [138], Copyright 2017, with permission from the authors, licensed under CC BY

organoids, irrespective of the presence or absence of liver organoids. Nevertheless, the cardiac beating rate and velocity decreased when cocultured with liver organoids, suggesting that clomipramine-induced cardiotoxicity is dependent on liver metabolism. This human organoids-on-chip system effectively mimics multiorgan physiology through the 3D coculture of liver and heart organoids, facilitating drug safety evaluation in a physiologically relevant manner. Bleomycin, an anticancer drug known for inducing lung fibrosis and inflammation, is believed to exert minimal effects on

liver and cardiac organoids. Skardal et al. developed a three-tissue OoC system comprising heart, liver, and lung organoids [128]. Each tissue construct was housed in modular microreactors designed for plug-and-play functionality and fabricated using conventional PDMS soft lithography and modeling techniques. Spherical liver organoids were generated using primary human hepatocytes, stellate cells, and Kupffer cells, whereas spherical cardiac organoids were formed from iPSCs. The lung modules consisted of lung fibroblasts, epithelial cells, and endothelial cells, with TEER

electrodes used to monitor the real-time barrier function. Bleomycin was administered on Day 3 and concluded on Day 9. Results showed that bleomycin decreased the compactness of the cardiac organoid morphology, although it did not halt cardiac organoid beating in a cardiac-only system (Fig. 4b). These findings suggest that bleomycin does not directly impact cardiac organoids but rather exerts side effects through cellular inflammatory factors. Ronaldson-Bouchard developed an advanced multiorgan tissue-chip system integrating the heart, liver, bone, and skin tissue niches, interconnected via a recirculating vascular flow to recapitulate organ-level functions [129]. Each tissue compartment was maintained in its optimized culture environment and separated from the common vascular flow by a selectively permeable endothelial barrier, ensuring physiological crosstalk without direct mixing. This system demonstrated remarkable stability, sustaining molecular, structural, and functional phenotypes for more than four weeks. To investigate multiorgan toxicity and miRNA changes, doxorubicin was used as a test drug in this system. Results revealed the presence of lower concentrations of doxorubicin in the heart chamber, whereas cardiac miRNA biomarkers exhibited significantly higher expression in the vascular circulation (Fig. 4c). This study demonstrated the potential of the system as a patient-specific model for the developmental testing of new therapeutic regimens and drug toxicity biomarkers.

The kidney plays a vital role in drug metabolism and excretion by filtering blood, removing waste products, and regulating electrolyte balance and fluid levels in the body [130]. Drug-induced nephrotoxicity is a prevalent issue that can result in acute renal failure. Hepatotoxicity and nephrotoxicity are two primary reasons for the withdrawal of drugs from the market [131]. Despite the close relationship between nephrotoxicity and liver metabolism, incorporating this factor into preclinical testing remains challenging due to the lack of adequate *in vitro* models. To address this challenge, Li et al. developed a multilayer chip with HepG2 cells on the upper layer and glomerular endothelial cells on the bottom layer to examine drug-induced toxic effects on kidney filtration [132]. Using ifosfamide (IFO) and verapamil (VER) as model drugs, they evaluated the nephrotoxicity of drugs after hepatic metabolism by measuring changes in cell viability, lactate dehydrogenase (LDH) leakage, and renal cell permeability to large protein molecules. This platform effectively captured drug metabolism in liver cells, and its biomimetic design characterized nephrotoxicity influenced by hepatic metabolic processes. In addition, Theobald et al. designed a chip that interconnected hepatic and kidney model systems to directly examine liver and liver-associated kidney toxicity [133]. Their results showed that compared with that in the static well-plate culture, albumin secretion and urea synthesis increased under microfluidic

on-chip culture conditions. They evaluated the effects of aflatoxin B1 (AFB1) and benzo[ $\alpha$ ] pyrene (B $\alpha$ P) on both liver and kidney tissue samples. However, this model primarily utilizes a limited number of cell types, which may not completely represent the complexities of organ interactions (Fig. 4d). Huang et al. also constructed a three-dimensional liver-kidney-on-a-chip with a biomimicking circulating system (LKOCBCS) for drug safety evaluation [134]. This system featured a parallel circulation model that mimics biological processes, allowing for the exchange of nutrients, compounds, and metabolites. It supported the coculture of 3D liver and renal proximal tubules with physiologically relevant circulation for up to seven days, stabilizing glucose concentration and cell metabolism. Cyclosporine A (CsA) serves as a model drug to evaluate hepatotoxicity and nephrotoxicity. Although this system successfully mimics normal tissue structure and function, a gap exists between engineered and native tissues, which could be addressed by advancing the 3D bioprinting technology. Recent developments in the field include the integration of advanced biomaterials and 3D bioprinting techniques, demonstrating promising potential for the creation of more physiologically relevant kidney and liver models.

The intestine plays a pivotal role in drug toxicity research using the OoC technology. As the primary site for nutrient absorption and the initial interface for orally administered pharmaceuticals, the intestine requires a comprehensive investigation of its interactions to achieve an appropriate evaluation of drug absorption, metabolism, and potential toxic effects. Intestine-on-a-chip models effectively replicate the intricate architecture and functionality of the human intestinal epithelium, including peristaltic movements, mucus production, and interactions with gut microbiota. These models have demonstrated significant potential in improving the predictability of drug toxicity and response, making them valuable tools for nonclinical pharmacotoxicology research. Moreover, gut-on-a-chip models are frequently used in combination with other organ chips, such as liver [135–137] and kidney [100] chips. For instance, Chen et al. developed a gut–liver coculture system to explore the interaction between these two organ systems under both normal and inflammatory conditions [138]. Unlike conventional PDMS-based designs, this platform was fabricated using polysulfone by micromachining. It featured unique characteristics, such as separate on-board, high-capacity, pulse-damped pumps for the circulation of culture medium within each individual microphysiological system (MPS) compartment, enabling microperfusion throughout the tissue. The system also included an independent oxygenation loop, improving the mass transfer on the basal side of the transwell through high-flow recirculation. The gut model incorporated enterocytes, goblet cells, and dendritic cells, whereas the liver model consisted of hepatocytes

and Kupffer cells. The functionality of the gut–liver system was maintained for two weeks, with gene expression and RNA sequencing analysis revealing the complex pathophysiological processes (Fig. 4e). Lucchetti et al. also constructed an MOoC platform that combined the human microbial-crosstalk (HuMix) gut-on-a-chip (GoC) with a dynamic liver-on-a-chip (LoC) to replicate the bidirectional interconnection between the gut and liver [139]. Using a colorectal cancer drug, they validated the capability of this platform to represent drug metabolism along the gut–liver axis, demonstrating it as a robust tool for exploring the intricate interplay between gut microbes and pharmaceuticals.

## 4.2 Drug toxicity evaluations in MOoC systems

Traditional toxicology models remain the primary approach for exploring chronic exposure. Although microfluidic systems have been developed to integrate up to three [140] or four [141] organs for *in vitro* investigations, these platforms are typically limited to short-term studies of acute metabolic functions, generally within a 48-h timeframe. In contrast, Oleaga et al. designed a cost-effective, flow-driven system that uses a rocker platform to generate shear stress across cell cultures [142]. This approach minimizes air bubble formation and promotes the even distribution of oxygen and nutrients throughout the devices. This system incorporates cardiac, liver, skeletal muscle, and neuronal cultures in a shared medium, sustaining them for up to two weeks. In drug development, the ventricular myocardium is widely used in cardiac modeling, and the liver is critical for regulating drug metabolism and drug half-life, potentially exerting side effects due to the accumulation of drugs or metabolites. Skeletal muscle, an essential glucose reservoir, is often affected by drugs, with side effects manifesting as tremors, spasms, atrophy, and muscle pain. The neuronal compartment, representing the nonfetal central nervous system (CNS), is included in this platform due to its sensitivity as a cellular system. Cardiac, liver, neuronal, and muscle tissues are all critical organs to evaluate in terms of toxicity, because adverse effects on these organs can compromise the viability of drug candidates. After 48 h of drug exposure, the platform evaluates the functionality of each organ by measuring heart beating frequency, muscle contractibility, neuronal electrophysiology, and liver-specific outputs such as albumin and urea production. This system was used to investigate the pharmacological toxicity of the following five drugs: doxorubicin, atorvastatin (ATR), valproic acid (VPA), acetaminophen (APAP), and a control compound, N-acetyl-m-aminophenol (AMAP). Remarkably, this platform is a pumpless system, making it both simple and cost-effective to use. It is also the first system to incorporate

both electrical and mechanical metrics for noninvasive, long-term monitoring of organ health, providing improved predictive capabilities for preclinical efficacy and toxicity research (Fig. 5a).

The effectiveness and safety of therapeutic candidates heavily depend on drug absorption and metabolism in the small intestine, metabolism within the liver, and excretion through the kidney. These processes play vital roles in the systemic distribution and elimination of drugs [143]. Nevertheless, traditional *in vitro* models lack the systemic interactions required for accurate drug testing. To address this problem, Maschmeyer et al. established a four-organ coculture microphysiological system that can be maintained for more than 28 days [144]. This platform integrates the following four human tissue equivalents: a 3D small intestine model, a skin biopsy, a 3D liver model for metabolism, and a kidney proximal tubule compartment for excretion. These tissues can maintain homeostasis over weeks, supported by two microphysiological fluid circuits and three reconstructed barriers. Each fluid flow circuit is powered by an independent on-chip peristaltic micropump. The chip features six air pressure connectors, four distinct culture compartments for tissues, and two reservoirs for collecting fluid from excretory organs. The micropump is integrated with the chip, and microchannels are connected to support pulsatile medium perfusion, which can substitute for the blood circuit. The intestinal barrier, proximal tubule barrier, and skin biopsy barrier are reconstructions. All tissues exhibited high cell viability and maintained a distinct physiological tissue structure throughout the coculture period. Furthermore, an in-depth analysis of metabolism and gene expression demonstrated the consistent establishment of homeostasis among all four tissue types for more than 28 days. This four-organ-chip aims to facilitate ADME profiling of drug candidates and conduct systemic toxicity testing of drug candidates through repeated dosing. Drug compounds are first absorbed by the intestine model, then pass to the skin and kidney equivalents via the simulated blood circulation, and finally reach the liver for distribution and metabolism within the liver. This platform effectively mimics drug absorption, first-pass metabolism, secondary metabolism, and excretion, allowing for an in-depth evaluation of pharmacokinetics and pharmacodynamics (Fig. 5b).

## 4.3 Multiorgan interactions in drug metabolism: beyond five-organ chips

Understanding the interactions between different organs within MOoC systems is pivotal for accurately modeling human physiological responses and drug effects. These systems provide a dynamic microenvironment that integrates multiple organs, enabling researchers to explore how drugs

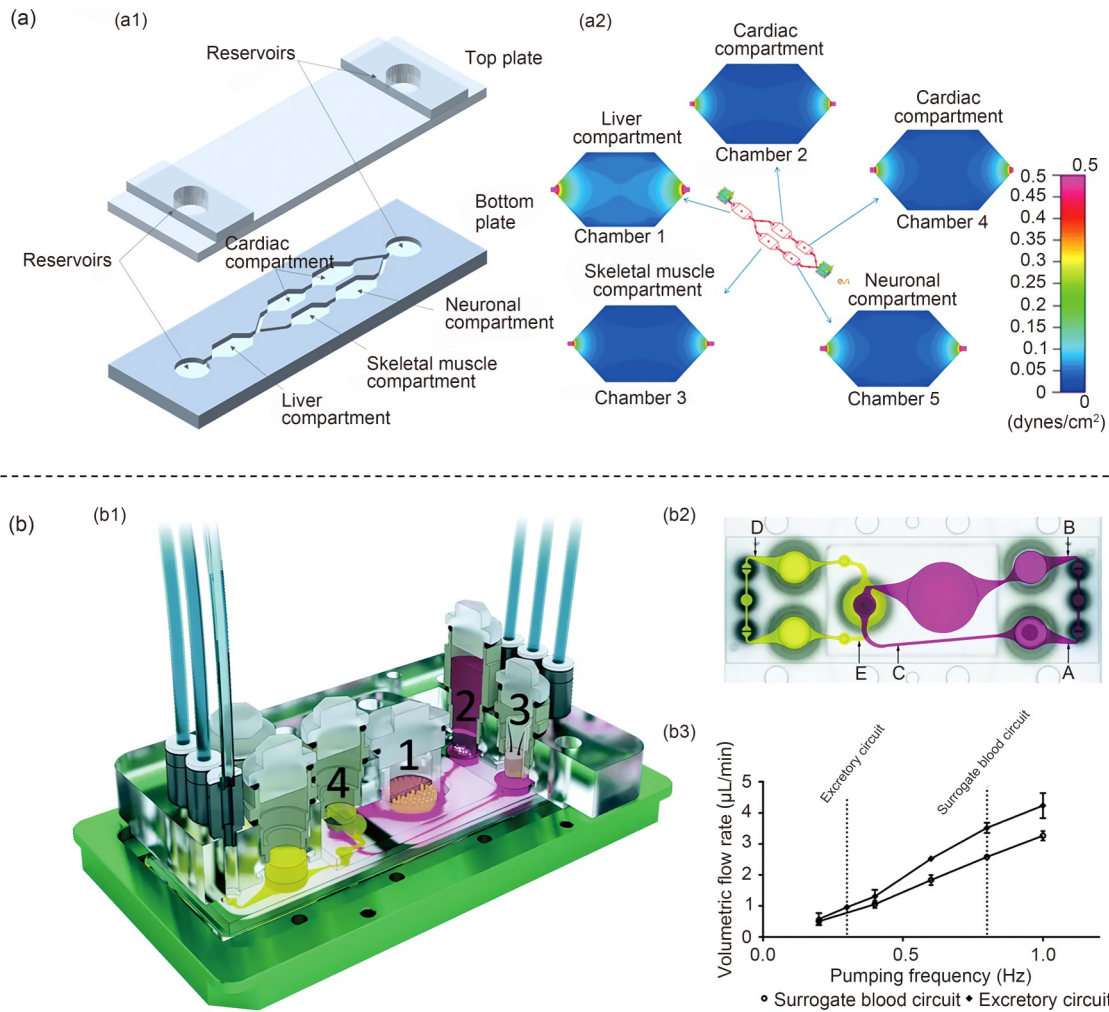


**Fig. 5** Drug toxicity in MOoC systems. (a) Schematic of the microfluidic platform incorporating cardiac, liver, skeletal muscle, and neuronal compartments, allowing for a 14-d culture period and the evaluation of five drugs simultaneously in this system. Reproduced from [142], Copyright 2016, with permission from the authors, licensed under CC BY. (b) Schematic of the four-organ microfluidic chip comprising the intestine, liver, skin, and kidney compartments, alongside a top-down view of the two microphysiological fluid flow circuits that simulate the drug absorption, distribution, metabolism, and excretion (ADME) model. Reproduced from [144], Copyright 2015, with permission from the authors, licensed under CC BY 3.0

are metabolized and exhibit interorgan interactions that contribute to their efficacy and toxicity. For instance, Rajan et al. developed an innovative MOoC system comprising six tissue constructs. The adhesive film-based microfluidic chip was developed using a cost-effective rapid-prototyping method involving patterned adhesive films. Microfluidic channels were generated by cutting double-sided adhesive films with a computer-controlled razor plotter [145]. Each chip consisted of four adhesive film layers designed for both three- and six-organoid systems. The three-organoid design featured discrete chambers connected by external tubing, whereas the six-organoid design included five interconnected chambers and an additional chamber that could be isolated for comparative studies. All organoids were bio-fabricated within the designated chamber, with the chip’s top side sealed using a PMMA lid. This platform was

capable of coculturing six organoids, including liver, cardiac, lung, endothelium, brain, and testes organoids, and supported cultures for up to 21 days. In particular, the system incorporated both human primary cells and iPSC-derived cells, which are arranged to mimic *in vivo* blood flow dynamics. Liver organoids were strategically positioned upstream to emulate their central role in drug metabolism. A key demonstration of the platform involved investigating the metabolism of the prodrug ifosfamide by the liver organoids, which produced chloroacetaldehyde, a toxic metabolite that caused neurotoxicity in downstream brain organoids. The study revealed a stark contrast between systems with or without the liver compartment. When 1 mmol/L ifosfamide was exposed in this system for seven days, the viability of brain organoids decreased in the presence of liver organoids, which was quantified by live/dead assays. In

contrast, no significant toxicity was detected in other organoids in the absence of liver organoids. These results emphasize the critical role of hepatic metabolism in mediating drug-induced toxicity (Fig. 6a). By incorporating organoids in a physiologically relevant sequence, the system effectively modeled reciprocal interactions between tissues, providing profound insights into drug metabolism, systemic toxicity, and interorgan crosstalk.

Human OoC systems represent a powerful tool for investigating complex drug metabolism, human physiological responses, and interorgan interactions under conditions that closely mimic *in vivo* conditions. Wang et al. developed a sophisticated human-on-a-chip platform incorporating seven-organ models, namely, the brain, pancreas, liver, lung, heart, gut, and endometrium, to explore the metabolite profiling and metabolomics of tolcapone, a drug approved for

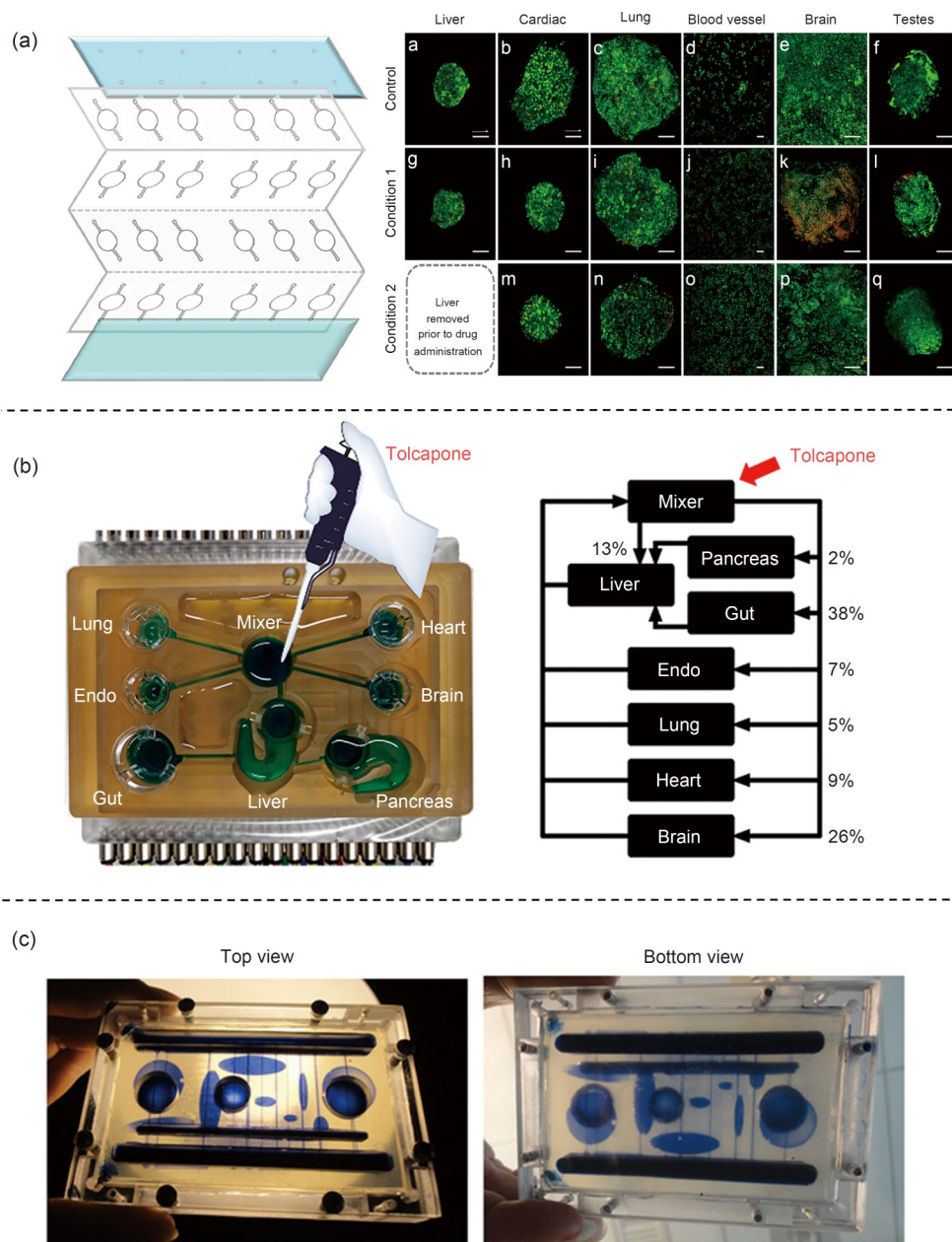


**Fig. 6** Drug interactions in MOoC systems. (a) A six-organ-on-a-chip platform used to examine the effects of ifosfamide across different organs. Reproduced from [145], Copyright 2020, with permission from Acta Materialia Inc. (b) The human-on-a-chip platform integrates seven interconnected microphysiological systems, representing the brain, pancreas, liver, lung, heart, gut, and endometrium. This system is used to explore the metabolite profiling and metabolomics of tolcapone. Reproduced from [146], Copyright 2019, with permission from the American Chemical Society. (c) Actual photographs of the two-layered pumpless body-on-a-chip device (14-chamber device) with trypan blue flowing through the channels and chambers. Reproduced from [148], Copyright 2016, with permission from Wiley Periodicals, Inc.

Parkinson's disease (PD) treatment [146]. The structure of the platform was divided into the following three functional layers: the top layer, made from polysulfone plastic, served as the fluidic circuit, ensuring the controlled flow of media; the middle layer, constructed from polyurethane, functioned as a selective membrane allowing molecular exchange; and the bottom layer, made of acrylic, acted as the pneumatic control system for fluid circulation and pressure regulation. Despite its clinical use for PD treatment, the impact of tolcapone on endogenous metabolites and metabolic pathways within the human CNS remains insufficiently explored. Metabolomics was used in this system to evaluate the metabolic characteristics and pathways in the human brain by liquid chromatography–mass spectrometry (LC-MS) after treatment with tolcapone. Through this system, 12 metabolites of tolcapone were identified, including three newly reported ones, which were associated with oxidation, reduction, and conjugation processes. The study also evaluated the effects of tolcapone on endogenous metabolic pathways in the brain OoC (Fig. 6b). This study represents a pioneering effort combining drug metabolism, energy metabolism, and cell engineering to investigate complex human physiology and multiorgan interactions. It emphasizes the potential of MPS platforms in comprehensive drug effect studies and understanding intricate human physiological processes.

Edington et al. developed a ten-organ-on-a-chip platform consisting of the liver, pancreas, gut, lung, heart, muscle, brain, endometrium, skin, and kidney, which maintained organ functionality for up to four weeks [147]. This platform enabled exploring the pharmacokinetic and pharmacodynamic (PKPD) properties of drugs. Because traditional PKPD models cannot be directly applied to multiorgan platforms, quantitative systems pharmacology (QSP) approaches were used instead. The QSP design considers each MPS, including the cell numbers and types, volumes of the work medium, and flow patterns. This platform can be used for preclinical drug development, allowing long-term culture (four weeks) with reliable fluidic and sampling operations. Miller et al. described another innovative multiorgan system, a pumpless 14-chamber platform representing 13 different tissues and organs, including both barrier and nonbarrier tissue chambers, to investigate the interactive responses among various cell lines [148]. The barrier chamber layer includes the skin, GI tract, and lungs, enabling direct exposure to chemical or biological agents (Fig. 6c). These agents can traverse a microfabricated membrane to enter nonbarrier chambers or the microfluidic circulation within the device. The nonbarrier chambers include fat, kidney, heart, adrenal glands, liver, spleen, pancreas, bone marrow, brain, and muscle. Using a programmable rocker platform to facilitate bidirectional fluid circulation, this pumpless system achieves flow through gravity induction. Pumpless systems provide several advantages, such as being economical, simplified in

setup and operation, and preventing bubbles from entering the chamber. In a 14-chamber device, five cell culture lines sustained high cellular activity (>85%) for seven days, demonstrating the ability of the system to sustain viable cultures. This model integrates multiple tissues and organs, enabling the study of interactive responses to drugs and chemicals across different organ systems in the human body, making it a powerful technique to evaluate the toxicity and efficacy of drugs.

## 5 Drug screening in MOoC systems

MOoC systems have gained significant attention in drug screening, particularly for small-molecule drugs, due to their ability to closely replicate human organ functions and interorgan interactions (Table 2). These platforms provide a more precise evaluation of drug efficacy and toxicity, bridging the gap between traditional 2D cell cultures and animal models by simulating complex organ-to-organ communication and drug responses. Although MOoC systems are not typically high-throughput due to their intricate designs and operational complexities, they serve as high-content models, providing detailed and comprehensive insights into the effects of drugs under physiologically relevant conditions [149]. There is extensive evidence on the effectiveness of these platforms in improving the predictive accuracy of human drug responses, especially for small-molecule drug discovery [150].

Small-molecule drugs are organic compounds with a molecular weight of less than 900 Da. Their relatively simple chemical structures enable easy synthesis and easy penetration into cell membranes, allowing interactions with intracellular targets [151]. These properties allow small-molecule drugs to inhibit protein synthesis, improve tumor immunogenicity, and counteract tumor-associated immunosuppression, thereby improving cancer immunotherapy strategies [152]. Furthermore, small-molecule drugs typically exert low off-target effects, making them a popular choice for cancer treatment [153]. OoC platforms are applied to investigate the absorption, metabolism, and distribution of small-molecule drugs, representing a more precise platform for drug screening, especially for CNS disorders. These disorders represent the second most common cause of death worldwide. Neurodegenerative diseases and brain cancers, which can affect individuals of all ages, are among the many that remain difficult to cure. Developing small-molecule drug delivery systems capable of penetrating the BBB is critical, because this barrier prevents most therapeutic agents from reaching the brain, significantly reducing the success rates of the development of small-molecule drugs [154, 155]. Therefore, it is necessary to develop a stable and precise model of BBB permeability for drug

evaluation. In this regard, Peng et al. developed a microfluidic-based human blood–brain barrier ( $\mu$ BBB) platform to predict the uptake of small-molecule drugs and nanoparticles (NPs) in the brain tissue targeting the CNS [156]. The platform integrates eight  $\mu$ BBB units, each comprising three distinct channels, namely, a blood channel lined with BBB cells (endothelial cells, pericytes, and astrocytes), a brain channel featuring a 3D glioblastoma multiforme (GBM) model, and a medium channel for the supply and exchange of nutrients (Fig. 7a). Immunofluorescence staining demonstrated that the platform accurately replicated the spatial organization of endothelial cells, pericytes, and astrocytes, mimicking the structure and functional characteristics of BBB. The  $\mu$ BBB platform provides both high-content and medium-throughput capabilities. Its high-content nature is reflected in its ability to extract and analyze detailed analytes from brain-like tissues using various methods, thus providing insights into drug–BBB interactions and permeability. Moreover, the platform achieves medium-throughput testing by incorporating multiple compounds under physiologically relevant conditions. Permeability coefficients were evaluated for various compounds, including high-molecular-weight dextran, the small hydrophilic molecule nitrofurantoin, the poorly permeable molecule sucrose, the lipophilic small molecule caffeine, and transport proteins for glucose and amino acids. The obtained results were consistent with established reports, demonstrating that this  $\mu$ BBB platform can accurately predict BBB permeability for small-molecule drugs, making it a powerful tool for CNS drug discovery and delivery studies.

Traditional high-throughput screening typically uses 2D cell monolayer cultures, typically performed in 96-well plates with liquid-dispensing and plate-handling robotics [157]. Nevertheless, cancer cells may lose their phenotypic characteristics over time in 2D cultures, significantly limiting the formation of tumor-like 3D structures [158, 159]. To overcome this limitation, Zhu et al. developed a dynamic microphysiological system chip platform (MSCP) with multiple functional microstructures [160]. This innovative platform integrates the intestine, liver, heart, and lung into a single microphysiological system, enabling the simultaneous evaluation of multiple anti-lung cancer drugs (Fig. 7b). The MSCP incorporates several advanced features, including a microvalve array that dynamically switches between organ formation and blood-flow modes, allowing the integration of up to four spheroids, either identical or varied, into a high-throughput drug testing model or microphysiological system. The MSCP is composed of three PDMS layers (microvalve layer, microchannel layer, and microwell layer) and five functional microstructures, including bubble buffer areas, latitudinal and longitudinal valve arrays, Galton nail plate-shaped micropillar arrays, and microwell arrays. The microvalve layer primarily consists of valve arrays oriented both latitudinally and longitudinally, whereas the microchannel layer features four longitudinal channels for cell injection and four latitudinal channels for drug injection, along with their respective inlets and outlets. There are 16 spheroid culture chambers along the longitudinal and latitudinal channels. The researchers generated high-throughput intestine (FHs 74 Int), liver (THLE-2), heart (HL-1), and lung cancer (A549) spheroids to evaluate drug absorption,

**Table 2** MOoC platforms for drug toxicity assessment and drug screening, as discussed in the text

| Classification | Description                     | Finding   | Drug   | Reference |
|----------------|---------------------------------|---|--|-----------|
| Drug toxicity  | Heart-liver-on-a-chip           | Evaluating cardiotoxicity with/without hepatocyte coculture; enabling noninvasive assessment of drug and metabolite through heart–liver crosstalk in vitro  | Cyclophosphamide   | [126]     |
|                | Liver-heart-on-a-chip           | Cardiac and liver organoids cultured in the upper chamber and bottom micropillar array, respectively; liver organoids demonstrating albumin/urea synthesis; cardiac organoids maintaining contractile function; used for antidepressant drug assessment | Clomipramine   | [127]     |
|                | Heart-liver-lung-on-a-chip      | Bioprinted liver and cardiac organoids integrated into a tissue-on-a-chip platform; combining bioengineered tissue models in a signal circulating perfusion system  | Bleomycin  | [128]     |
|                | Heart-liver-bone-skin-on-a-chip | Interconnected organs via recirculating vascular flow, with each tissue maintained in its optimized microenvironment and isolated from the shared circulation by selective endothelial barriers   | Doxorubicin  | [129]     |
|                | Liver-kidney-on-a-chip          | Enabling the simultaneous assessment of hepatic drug metabolism and renal toxicity in a single device   | Ifosfamide; verapamil  | [132]     |
|                | Liver-kidney-on-a-chip          | A two-chamber interconnected biochip culturing liver and kidney cells, allowing bidirectional transport of drug metabolites between chambers via convective flow  | Aflatoxin B1 (AFB1); benzo[ $\alpha$ ] pyrene (B $\alpha$ P) | [133]     |

To be continued

Table 2 (continued)

| Classification | Description  | Finding  | Drug  | Reference |
|----------------|--|--|---|-----------|
|                | Liver-kidney-on-a-chip                                 | 3D liver–kidney organ-on-a-chip with a biomimicking circulating system (LKOCBCS); parallel microfluidic circulatory system consisting of 3D biomimetic liver lobule and renal proximal tubule barrier models; multiorgan toxicity/pharmacokinetics studies   | Cyclosporine A (CsA)  | [134]     |
|                | Gut-liver-on-a-chip                                    | A multiorgan platform coculturing hepatic and intestinal cells to investigate gut–liver axis interactions under both physiological and inflammatory conditions   | –   | [138]     |
|                | Gut-liver-on-a-chip                                    | A human microbial-crosstalk (HuMix) gut-on-a-chip (GoC) model coupled with Dynamic42 liver-on-a-chip (LoC) which models the gut–liver axis, enabling the investigation of microbial influences on drug metabolism  | Irinotecan  | [139]     |
|                | Cardiac/muscle/<br>neuronal/liver module-<br>on-a-chip | A modular, reconfigurable system under continuous flow conditions using serum-free defined medium in a pumpless platform for 14 days; five drugs evaluated   | Doxorubicin; atorvastatin (ATR); valproic acid (VPA); acetaminophen (APAP); N-acetyl-m-aminophenol (AMAP) | [142]     |
|                | Intestine-skin-liver-<br>kidney-on-a-chip              | A system comprising two microphysiological fluid circuits and three reconstructed barriers, maintaining tissue homeostasis for more than 28 days and enabling ADME and systemic toxicity studies   | –   | [144]     |
|                | Six-organ-on-a-chip                                    | A system integrating six humanized constructs (liver, cardiac, lung, endothelium, brain, and testes organoids) in a shared circulatory network, maintaining high viability for 21 days to study multi-tissue interactions  | Ifosfamide  | [145]     |
|                | Seven-organ-on-a-chip                                  | Seven interconnected microphysiological systems (MPSs) comprising brain, pancreas, liver, lung, heart, gut, and endometrium tissue models; representing the first comprehensive evaluation of metabolic signatures and pathway dynamics in a human-on-a-chip system  | Tolcapone   | [146]     |
|                | Ten-organ-on-a-chip                                    | Ten MPS platform (liver, pancreas, gut, lung, heart, muscle, brain, endometrium, skin, kidney) with sustained multi-tissue interactions for more than four weeks; integrated with quantitative systems pharmacology (QSP) computational modeling to simulate the distribution of endogenous metabolites and in vitro pharmacokinetics; high-throughput capacity, long-term stability, and high degree-of-freedom (DOF) | Diclofenac (DCF)  | [147]     |
|                | Thirteen-organ-on-a-chip                               | “Body-on-a-chip” platform features: 14 chamber designs (13 organs), barrier tissues (skin, GI tract, and lungs), and nonbarrier tissues (fat, kidney, heart, adrenal glands, liver, spleen, pancreas, bone marrow, brain, and muscle); gravity-driven fluidics for interorgan crosstalk studies; applications: multi-tissue interaction analysis under a controlled microenvironment                                   | –   | [148]     |
| Drug screening | Human blood–brain barrier (BBB) platform               | A platform integrating eight microfluidic-based blood–brain barrier ( $\mu$ BBB) units, enabling high-content analysis of cellular interactions and medium-throughput screening for drug permeability studies  | Small-molecule drugs  | [156]     |
|                | Microphysiological system chip platform (MSCP)         | High-throughput 3D cancer spheroid model; four-organ (intestine–liver–heart–lung) coculture system; parallel evaluation of four anti-lung cancer drugs   | Anti-lung cancer drugs (cisplatin, pemetrexed, doxorubicin, and docetaxel)                                | [160]     |
|                | Micropillar/microwell chip                             | Containing brain tumor cells and three primary brain cancer cells; high-throughput biochemical and cell-based efficacy assays; antitumor drug evaluation and mechanism studies   | Twenty-four therapeutic anticancer drugs  | [161]     |

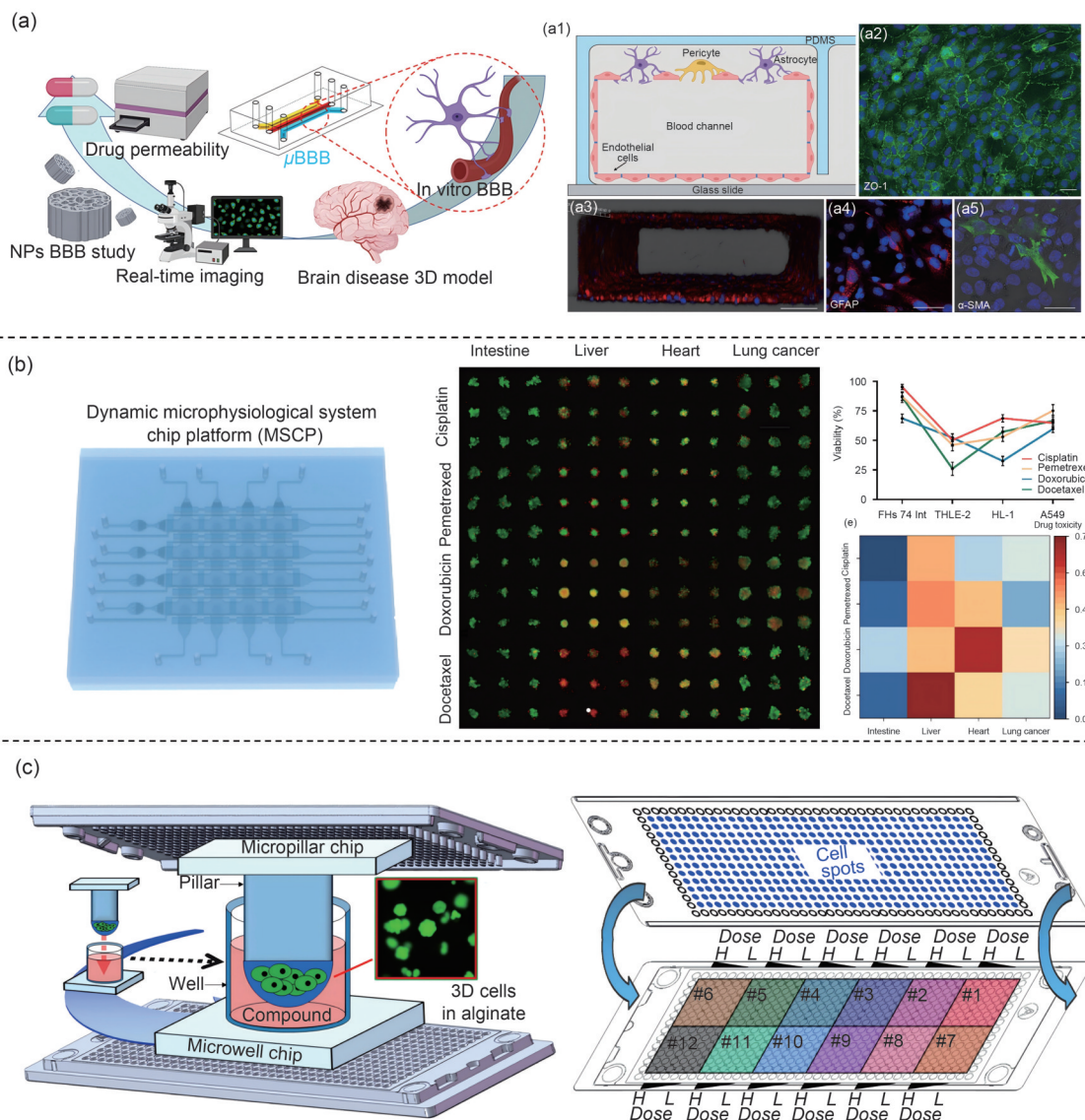


**Fig. 7** MOoC for drug screening. (a) The microfluidic-based human blood–brain barrier ( $\mu$ BBB) system mimics and predicts the uptake of small molecules and nanoparticles (NPs) targeting the central nervous system: (a1) a schematic side view of the  $\mu$ BBB; (a2, a3) immunofluorescence images of the tight junction protein ZO-1 (green) and the vessel-like structure (red); (a4, a5) immunofluorescence images of astrocytes stained for GFAP (red) and pericytes labeled for  $\alpha$ -SMA (green). Reproduced from [156], Copyright 2020, with permission from the American Chemical Society. (b) A high-throughput microphysiological system incorporating intestine, liver, heart, and lung cancer tissues, which is designed to investigate the effects of four different drugs simultaneously. The rightmost panel displays the drug response profiles, where compounds sequentially perfuse through intestine, liver, and heart spheroids before reaching the lung cancer spheroids. Reproduced from [160], Copyright 2024, with permission from the authors, licensed under CC BY-NC-ND. (c) Schematic of a micropillar and microwell chip platform used for anticancer drug screening. The right panel depicts the configuration of the micropillar/microwell chip, which was designed for the parallel screening of 12 drugs in a single assay. Reproduced from [161], Copyright 2013, with permission from the American Chemical Society

metabolism, and side effects. By staining specific proteins and measuring the size of the four spheroids, they established a microphysiological system for evaluating oral anti-lung cancer drugs within 48 h. Furthermore, the four spheroids maintained high viability for up to five days. The anticancer effects of the four drugs cisplatin, docetaxel, pemetrexed, and doxorubicin were evaluated using the A549 non-small cell lung cancer epithelial cell line. Live/dead and cell viability assays showed that doxorubicin exhibited the

strongest anticancer efficacy, followed by cisplatin, docetaxel, and pemetrexed. These results demonstrate the high-throughput capabilities of MSCP in rapidly and efficiently generating drug evaluation data and also maintaining physiologically relevant conditions. Lee et al. developed a miniaturized micropillar/microwell chip that supports primary human cells for drug screening and enables convenient medium exchange by replacing the cell-containing micropillar/microwell chip with a medium-containing microwell

chip [161]. This platform contained 12 regions, each with a 6×6 miniarray, allowing the assessment of six different drug doses. A total of 24 therapeutic anticancer drugs were tested on this chip using the U251 brain cancer cell line and three primary brain cancer cells obtained from patients. Their study demonstrated that the micropillar/microwell chip represents a promising, high-throughput, and microscale alternative to traditional *in vitro* multi-well plate platforms, providing novel opportunities for rapid and cost-effective evaluation of drug efficacy in the early stages of clinical studies for individual patients with cancer (Fig. 7c).

## 6 Challenges and perspectives

The primary goal of MOoC systems is to accurately replicate the structure, function, and microphysiology of organs and their interorgan interactions *in vitro*, thus mimicking *in vivo* conditions. Since the introduction of the OoC concept in the 2000s, this technology has rapidly evolved and gained significant traction as a promising alternative to traditional animal models in drug development [162]. Despite its potential, the field remains in its nascent stages and faces various challenges, including complexity and integration, lack of standardization, reproducibility concerns, and the need for a multidisciplinary approach.

In the MOoC system, biosensors, including optical sensors, mechanical sensors, and electrochemical sensors, hold the key to real-time, noninvasive monitoring of various physiological parameters and molecular events occurring within the chip. These sensors can dynamically adjust to experimental conditions, similar to the body's own regulatory mechanisms responding to changing internal states [163]. Nevertheless, biosensors must be scaled down to fit within the microfluidic channels and chambers of the MOoC without sacrificing their performance. In the future, with the advancement of nanotechnology and microfabrication techniques, nanoscale biosensors can be developed to achieve high sensitivity and specificity and also to maintain a small footprint.

Although the OoC technology constitutes a more accurate representation of human organ environments than conventional models, it faces substantial hurdles in replicating the intricate interactions found within human tissues. This complexity involves integrating multiple cell types, ECM components, and the dynamic mechanical forces that characterize biological systems. MOoC systems are designed to incorporate various cell types within a single device, creating a physiological environment that closely resembles human tissues. Importantly, these multiorgan platforms uniquely enable the maintenance of systemic homeostasis through dynamic feedback mechanisms between interconnected tissue modules, a capability demonstrated in models

of gut–liver–kidney metabolic coordination [164]. This self-regulatory capacity positions MOoC as a critical tool for investigating chronic diseases and long-term drug responses that require weeks to months of stable culture conditions. Nevertheless, each cell type has specific requirements concerning the culture medium and growth characteristics, including growth time and maturity. Effectively assembling and seeding these cells to mimic their natural environments poses a significant challenge.

A parallel challenge lies in incorporating nervous or immune components to better mimic human pathophysiology. Immune cells play a vital role in the body's responses to cancer and overall physiological homeostasis. Adding immunocompetent elements to MOoC systems is essential for better recapitulating the *in vivo* pathophysiology. For instance, T cells, a key component of the adaptive immune system, are highly relevant in cancer immunotherapy. Nevertheless, integrating them into MOoC architectures is complex. Current efforts have achieved some progress in establishing models with resident macrophages, such as in gut–liver axis inflammation research [138]. This model provides insights into how local immune responses in these two organs can affect inflammatory conditions. It provides a useful platform for clarifying the underlying mechanisms of disease progression. The nervous system exerts a profound impact on organ function and overall homeostasis. In recent years, there have been some initial attempts to incorporate neuronal networks into MOoC systems. For instance, in gut–liver–cerebral interactions in the context of PD [165], gut–liver MPS and brain MPS were circulated with a common culture medium containing immune cells. This system demonstrated interorgan interactions in the context of PD. However, creating hierarchically organized neural circuits that can accurately recapitulate the complexity of the *in vivo* nervous system has not yet been achieved. Future studies should focus on developing methods to grow and integrate more complex neural circuits into MOoC systems.

Ensuring consistency across laboratories and experiments is crucial for the credibility of MOoC technology. Variations in chip fabrication, cell sourcing, and experimental conditions can result in inconsistent outcomes, complicating data comparison and validation across studies. Therefore, it is crucial to streamline and simplify complex MOoC systems for drug screening. The key factors for improving standardization include chip size, cell density, sourcing of cell lines, metabolic rates, monitoring methods, and detection parameters. By addressing these factors, the reproducibility of the MOoC system can be improved, fostering wider adoption and acceptance in pharmaceutical research and development.

The longevity of MOoC systems is also a pivotal factor, particularly for modeling chronic conditions and investigating long-term drug effects. Chronic conditions such as

diabetes, cardiovascular diseases, neurodegenerative disorders, and chronic inflammation evolve over months or even years. To accurately simulate these disease processes, MOoC platforms must sustain organ-specific physiological functions and interorgan communication over prolonged periods. For instance, modeling diabetic complications requires the continuous observation of metabolic and inflammatory signals between multiple organ systems. Without this sustained functionality, it may be difficult to accurately capture the dynamics of disease progression and the cumulative effects of therapeutic interventions. Similarly, the evaluation of long-term drug efficacy and chronic toxicity requires sustained system stability. Drugs targeting chronic conditions often exert delayed therapeutic effects or adverse reactions that manifest over weeks or months, and MOoC systems must maintain functionality over such timeframes.

As the MOoC technology advances, it holds significant promise for transforming personalized medicine. Personalized medicine represents a paradigm shift in healthcare, focusing on customized medical treatment based on the unique characteristics of each patient. This approach goes beyond a one-size-fits-all model by considering a patient's genetic profile, environmental influences, and lifestyle factors to develop individualized treatment plans. Recent breakthroughs in iPSC differentiation technology have made it feasible to develop personalized MOoC systems. Using this method, patient-derived cells can be reprogrammed into iPSCs and differentiated into target organs. Through the use of patient-specific cells, MOoCs can be tailored to examine individual responses to drugs, thus paving the way for more personalized and effective treatment regimens. Moreover, personalized MOoC systems are not limited to modeling normal cellular functions; they can replicate the specific cellular environments of individual patients, allowing for more accurate predictions of how these individuals will respond to various drug treatments. This approach reduces the risks of adverse effects and increases the probability of successful outcomes. Furthermore, the personalized nature of MOoC systems opens new avenues in the development of regenerative medicine and cell-based therapies. By leveraging patient-specific cells, these therapies can directly target the underlying cellular mechanisms of the disease, potentially resulting in more lasting and effective treatments. Personalized MOoC systems provide a profound opportunity to address diseases at their root causes, representing a leap forward in tailored medical interventions.

Another promising frontier that improves the capabilities of MOoC systems lies in their integration with big data analytics, artificial intelligence (AI), and emerging synthetic biology tools. This convergence holds revolutionary potential for healthcare, particularly in drug discovery, precision medicine, and point-of-care diagnostics. AI-driven experimental

optimization now enables the dynamic adjustment of fluid flow rates, oxygen gradients, or nutrient concentrations to better mimic human pathophysiology. Moreover, multi-modal data integration approaches enable the synthesis of diverse biological datasets, including imaging, omics, and physiological parameters, to build high-fidelity models that precisely capture cellular dynamics [166]. The extensive data generated by MOoC experiments serve as a rich source of biological information. When analyzed through big data technology, these datasets can reveal previously hidden patterns and insights. AI, particularly machine learning algorithms, can further augment this data interpretation by learning from complex datasets and producing accurate predictions [167]. The combination of MOoC systems with these advanced technologies could dramatically accelerate the pace of drug discovery [168]. For instance, AI can analyze the vast and intricate datasets generated from MOoC experiments, thereby pinpointing potential drug candidates more efficiently. Machine learning models trained on these datasets can predict the effects of drug compounds on human tissues with greater reliability, allowing researchers to evaluate the efficacy and safety of these compounds long before they reach the clinical trial stage. This predictive capability can significantly reduce both the time and financial costs associated with drug development by identifying viable compounds early in the process and filtering out those likely to fail. In addition, AI can accelerate high-throughput screening of drugs on MOoC. The integration of big data, AI, synthetic biology, and MOoC technology also promises to advance personalized medicine [169]. By analyzing a patient's genetic, environmental, and lifestyle information in conjunction with MOoC data, AI algorithms can predict individual responses to specific treatments. This personalized approach ensures that therapies are tailored to each patient, maximizing effectiveness and minimizing adverse effects. In precision oncology, AI technology combined with the CRISPR-Cas9 system allows the prediction of guide RNA (gRNA) on-target and off-target activity. This integration not only holds considerable promise but also has several challenges [170]. AI technology, particularly deep-learning-based models, can sift through large-scale genomic sequences to predict the probability of a gRNA binding to its intended on-target site [171]. However, accurately predicting off-target activity remains a formidable challenge. Synthetic biology provides novel methods to improve the AI-CRISPR-Cas9 system in precision oncology. Synthetic biology techniques can be used to engineer gRNAs with modified backbones or chemical modifications. These modifications can be guided by AI-derived insights on how to improve the stability and specificity of gRNA–DNA interactions [172]. In conclusion, the synergy among MOoC technology, AI, and programmable biological tools represents a paradigm shift in biomedicine. This convergence

accelerates therapeutic development cycles, which is a true hallmark of next-generation biomedical innovation.

## 7 Conclusions

MOoC technology marks a significant breakthrough in microfluidic systems, providing an advanced platform for simulating intricate physiological interactions and streamlining drug development. By incorporating multiple organ models, these devices deliver a more realistic representation of human physiology, thereby improving the predictability of drug efficacy and toxicity.

**Acknowledgements** This work was financially supported by the National Natural Science Foundation of China (No. 32371475) and the Natural Science Foundation of Jiangsu Province, Major Project (No. BK20222008).

**Author contributions** LQ: conceptualization, original draft preparation, and review and editing. SQC and LZ: review and editing. FZ and CC: visualization and review and editing. NPH: conceptualization, review and editing, supervision, and funding acquisition.

## Declarations

**Conflict of interest** The authors declare that they have no conflict of interest.

**Ethical approval** This article does not contain any studies with human or animal subjects performed by any of the authors.

## References

- Begley CG, Ellis LM (2012) Drug development: raise standards for preclinical cancer research. *Nature* 483(7391):531–533. <https://doi.org/10.1038/483531a>
- Liu X, Zheng W, Jiang X (2019) Cell-based assays on microfluidics for drug screening. *ACS Sens* 4(6):1465–1475. <https://doi.org/10.1021/acssensors.9b00479>
- Skardal A, Shupe T, Atala A (2016) Organoid-on-a-chip and body-on-a-chip systems for drug screening and disease modeling. *Drug Discov Today* 21(9):1399–1411. <https://doi.org/10.1016/j.drudis.2016.07.003>
- Li YH, Meng Q, Yang MB et al (2019) Current trends in drug metabolism and pharmacokinetics. *Acta Pharm Sin B* 9(6):1113–1144. <https://doi.org/10.1016/j.apsb.2019.10.001>
- Ong LJY, Chia S, Wong SQR et al (2022) A comparative study of tumour-on-chip models with patient-derived xenografts for predicting chemotherapy efficacy in colorectal cancer patients. *Front Bioeng Biotechnol* 10:952726. <https://doi.org/10.3389/fbioe.2022.952726>
- Tang QQ, Li XY, Lai C et al (2021) Fabrication of a hydroxyapatite-PDMS microfluidic chip for bone-related cell culture and drug screening. *Bioact Mater* 6(1):169–178. <https://doi.org/10.1016/j.bioactmat.2020.07.016>
- Wasalathanthri DP, Li DD, Song DH et al (2015) Elucidating organ-specific metabolic toxicity chemistry from electrochemiluminescent enzyme/DNA arrays and bioreactor bead-LC-MS/MS. *Chem Sci* 6(4):2457–2468. <https://doi.org/10.1039/c4sc03401e>
- Criscione J, Rezaei Z, Hernandez Cantu CM et al (2023) Heart-on-a-chip platforms and biosensor integration for disease modeling and phenotypic drug screening. *Biosens Bioelectron* 220:114840. <https://doi.org/10.1016/j.bios.2022.114840>
- Zhang Y, Wang X, Yang Y et al (2023) Recapitulating essential pathophysiological characteristics in lung-on-a-chip for disease studies. *Front Immunol* 14:1093460. <https://doi.org/10.3389/fimmu.2023.1093460>
- Wilmer MJ, Ng CP, Lanz HL et al (2016) Kidney-on-a-chip technology for drug-induced nephrotoxicity screening. *Trends Biotechnol* 34(2):156–170. <https://doi.org/10.1016/j.tibtech.2015.11.001>
- Hassan S, Sebastian S, Maharjan S et al (2020) Liver-on-a-chip models of fatty liver disease. *Hepatology* 71(2):733–740. <https://doi.org/10.1002/hep.31106>
- Xian C, Zhang J, Zhao S et al (2023) Gut-on-a-chip for disease models. *J Tissue Eng* 14:1–14. <https://doi.org/10.1177/20417314221149882>
- Sung JH, Wang YI, Sriram NN et al (2019) Recent advances in body-on-a-chip systems. *Anal Chem* 91(1):330–351. <https://doi.org/10.1021/acs.analchem.8b05293>
- Dehne EM, Hasenberg T, Marx U (2017) The ascendance of microphysiological systems to solve the drug testing dilemma. *Future Sci OA* 3(2):FSO0185. <https://doi.org/10.4155/fsoa-2017-0002>
- Khodabukus A, Madden L, Prabhu NK et al (2019) Electrical stimulation increases hypertrophy and metabolic flux in tissue-engineered human skeletal muscle. *Biomaterials* 198:259–269. <https://doi.org/10.1016/j.biomaterials.2018.08.058>
- Kaarj K, Yoon JY (2019) Methods of delivering mechanical stimuli to organ-on-a-chip. *Micromachines* 10(10):E700. <https://doi.org/10.3390/mi10100700>
- Kumar V, Perikamana SKM, Tata A et al (2022) An in vitro microfluidic alveolus model to study lung biomechanics. *Front Bioeng Biotechnol* 10:848699. <https://doi.org/10.3389/fbioe.2022.848699>
- Hsieh HL, Nath P, Huang JH (2019) Multistep fluidic control network toward the automated generation of organ-on-a-chip. *ACS Biomater Sci Eng* 5(9):4852–4860. <https://doi.org/10.1021/acsbomaterials.9b00912>
- Chen FM, Zhang M, Wu ZF (2010) Toward delivery of multiple growth factors in tissue engineering. *Biomaterials* 31(24):6279–6308. <https://doi.org/10.1016/j.biomaterials.2010.04.053>
- Ahadian S, Civitarese R, Bannerman D et al (2018) Organ-on-a-chip platforms: a convergence of advanced materials, cells, and microscale technologies. *Adv Healthc Mater* 7(2):1700506. <https://doi.org/10.1002/adhm.201700506>
- Esch MB, Ueno H, Applegate DR et al (2016) Modular, pumpless body-on-a-chip platform for the co-culture of GI tract epithelium and 3D primary liver tissue. *Lab Chip* 16(14):2719–2729. <https://doi.org/10.1039/c6lc00461j>
- Benam KH, Villenave R, Lucchesi C et al (2016) Small airway-on-a-chip enables analysis of human lung inflammation and drug responses in vitro. *Nat Methods* 13(2):151–157. <https://doi.org/10.1038/nmeth.3697>
- Jang KJ, Mehr AP, Hamilton GA et al (2013) Human kidney proximal tubule-on-a-chip for drug transport and nephrotoxicity assessment. *Integr Biol* 5(9):1119–1129. <https://doi.org/10.1039/C3IB40049B>
- Achyuta AKH, Conway AJ, Crouse RB et al (2013) A modular

- approach to create a neurovascular unit-on-a-chip. *Lab Chip* 13(4):542–553.  
<https://doi.org/10.1039/c2lc41033h>
25. Rozman M, Štukovnik Z, Sušnik A et al (2022) A HepG2 cell-based biosensor that uses stainless steel electrodes for hepatotoxin detection. *Biosensors* 12(3):160.  
<https://doi.org/10.3390/bios12030160>
  26. Lee H, Jung KB, Kwon O et al (2022) *Limosilactobacillus reuteri* DS0384 promotes intestinal epithelial maturation via the postbiotic effect in human intestinal organoids and infant mice. *Gut Microbes* 14(1):2121580.  
<https://doi.org/10.1080/19490976.2022.2121580>
  27. Csöbörnyeiová M, Polák Š, Danišovič L (2016) Toxicity testing and drug screening using iPSC derived hepatocytes, cardiomyocytes, and neural cells. *Can J Physiol Pharmacol* 94(7):687–694.  
<https://doi.org/10.1139/cjpp-2015-0459>
  28. Sanchez-Freire V, Lee AS, Hu SJ et al (2014) Effect of human donor cell source on differentiation and function of cardiac induced pluripotent stem cells. *J Am Coll Cardiol* 64(5):436–448.  
<https://doi.org/10.1016/j.jacc.2014.04.056>
  29. Sun N, Panetta NJ, Gupta DM et al (2009) Feeder-free derivation of induced pluripotent stem cells from adult human adipose stem cells. *Proc Natl Acad Sci USA* 106(37):15720–15725.  
<https://doi.org/10.1073/pnas.0908450106>
  30. Kloos D, Lachmann N (2022) Generation of human iPSC from small volume peripheral blood samples. *Methods Mol Biol* 2429:27–39.  
[https://doi.org/10.1007/978-1-0716-1979-7\\_3](https://doi.org/10.1007/978-1-0716-1979-7_3)
  31. Zhou T, Benda C, Dunzinger S et al (2012) Generation of human induced pluripotent stem cells from urine samples. *Nat Protoc* 7(12):2080–2089.  
<https://doi.org/10.1038/nprot.2012.115>
  32. Ingber DE (2022) Human organs-on-chips for disease modelling, drug development and personalized medicine. *Nat Rev Genet* 23(8):467–491.  
<https://doi.org/10.1038/s41576-022-00466-9>
  33. Thompson CL, Fu S, Knight MM et al (2020) Mechanical stimulation: a crucial element of organ-on-chip models. *Front Bioeng Biotechnol* 8:602646.  
<https://doi.org/10.3389/fbioe.2020.602646>
  34. Kaarj K, Madias M, Akarapipad P et al (2020) Paper-based in vitro tissue chip for delivering programmed mechanical stimuli of local compression and shear flow. *J Biol Eng* 14:20.  
<https://doi.org/10.1186/s13036-020-00242-5>
  35. Zheng Y, Chen JM, Craven M et al (2012) In vitro microvessels for the study of angiogenesis and thrombosis. *Proc Natl Acad Sci USA* 109(24):9342–9347.  
<https://doi.org/10.1073/pnas.1201240109>
  36. Lee PJ, Hung PJ, Lee LP (2007) An artificial liver sinusoid with a microfluidic endothelial-like barrier for primary hepatocyte culture. *Biotechnol Bioeng* 97(5):1340–1346.  
<https://doi.org/10.1002/bit.21360>
  37. Vickerman V, Kamm RD (2012) Mechanism of a flow-gated angiogenesis switch: early signaling events at cell–matrix and cell–cell junctions. *Integr Biol* 4(8):863–874.  
<https://doi.org/10.1039/c2ib00184e>
  38. Kim HJ, Huh D, Hamilton G et al (2012) Human gut-on-a-chip inhabited by microbial flora that experiences intestinal peristalsis-like motions and flow. *Lab Chip* 12(12):2165–2174.  
<https://doi.org/10.1039/C2LC40074J>
  39. Liu XF, Yu JQ, Dalan R et al (2014) Biological factors in plasma from diabetes mellitus patients enhance hyperglycaemia and pulsatile shear stress-induced endothelial cell apoptosis. *Integr Biol* 6(5):511–522.  
<https://doi.org/10.1039/C3IB40265G>
  40. Stucki AO, Stucki JD, Hall SRR et al (2015) A lung-on-a-chip array with an integrated bio-inspired respiration mechanism. *Lab Chip* 15(5):1302–1310.  
<https://doi.org/10.1039/C4LC01252F>
  41. Bein A, Shin W, Jalili-Firoozinezhad S et al (2018) Microfluidic organ-on-a-chip models of human intestine. *Cell Mol Gastroenterol Hepatol* 5(4):659–668.  
<https://doi.org/10.1016/j.jcmgh.2017.12.010>
  42. Tomasek JJ, Gabbiani G, Hinz B et al (2002) Myofibroblasts and mechano-regulation of connective tissue remodelling. *Nat Rev Mol Cell Biol* 3(5):349–363.  
<https://doi.org/10.1038/nrm809>
  43. Zhang BY, Korolj A, Lai BFL et al (2018) Advances in organ-on-a-chip engineering. *Nat Rev Mater* 3(8):257–278.  
<https://doi.org/10.1038/s41578-018-0034-7>
  44. Bilek AM, Dee KC, Gaver DP III (2003) Mechanisms of surface-tension-induced epithelial cell damage in a model of pulmonary airway reopening. *J Appl Physiol* 94(2):770–783.  
<https://doi.org/10.1152/jappphysiol.00764.2002>
  45. Dixon JB, Raghunathan S, Swartz MA (2009) A tissue-engineered model of the intestinal lacteal for evaluating lipid transport by lymphatics. *Biotechnol Bioeng* 103(6):1224–1235.  
<https://doi.org/10.1002/bit.22337>
  46. Zhao YM, Rafatian N, Wang EY et al (2020) Engineering microenvironment for human cardiac tissue assembly in heart-on-a-chip platform. *Matrix Biol* 85:189–204.  
<https://doi.org/10.1016/j.matbio.2019.04.001>
  47. Velasco-Mallorquí F, Fernández-Costa JM, Neves L et al (2020) New volumetric CNT-doped gelatin-cellulose scaffolds for skeletal muscle tissue engineering. *Nanoscale Adv* 2(7):2885–2896.  
<https://doi.org/10.1039/d0na00268b>
  48. Sei Y, Justus K, LeDuc P et al (2014) Engineering living systems on chips: from cells to human on chips. *Microfluid Nanofluid* 16(5):907–920.  
<https://doi.org/10.1007/s10404-014-1341-y>
  49. Kuczynski B, Ruder WC, Messner WC et al (2009) Probing cellular dynamics with a chemical signal generator. *PLoS ONE* 4(3):e4847.  
<https://doi.org/10.1371/journal.pone.0004847>
  50. Kim Y, Joshi SD, Messner WC et al (2011) Detection of dynamic spatiotemporal response to periodic chemical stimulation in a *Xenopus* embryonic tissue. *PLoS ONE* 6(1):e14624.  
<https://doi.org/10.1371/journal.pone.0014624>
  51. Huh D, Hamilton GA, Ingber DE (2011) From 3D cell culture to organs-on-chips. *Trends Cell Biol* 21(12):745–754.  
<https://doi.org/10.1016/j.tcb.2011.09.005>
  52. Maaskant E, Tempelman K, Benes NE (2018) Hyper-cross-linked thin polydimethylsiloxane films. *Eur Polym J* 109:214–221.  
<https://doi.org/10.1016/j.eurpolymj.2018.09.052>
  53. Harun-Ur-Rashid M, Jahan I, Foyez T et al (2023) Bio-inspired nanomaterials for micro/nanodevices: a new era in biomedical applications. *Micromachines* 14(9):1786.  
<http://doi.org/10.3390/mi14091786>
  54. Auner AW, Tasneem KM, Markov DA et al (2019) Chemical-PDMS binding kinetics and implications for bioavailability in microfluidic devices. *Lab Chip* 19(5):864–874.  
<https://doi.org/10.1039/C8LC00796A>
  55. Lyra-Leite DM, Andres AM, Cho N et al (2019) Matrix-guided control of mitochondrial function in cardiac myocytes. *Acta Biomater* 97:281–295.  
<https://doi.org/10.1016/j.actbio.2019.08.007>
  56. Liu J, Zheng HY, Dai XY et al (2020) Transparent PDMS bioreactors for the fabrication and analysis of multi-layer

- pre-vascularized hydrogels under continuous perfusion. *Front Bioeng Biotechnol* 8:568934.  
<https://doi.org/10.3389/fbioe.2020.568934>
57. Campbell SB, Wu QH, Yazbeck J et al (2021) Beyond polydimethylsiloxane: alternative materials for fabrication of organ-on-a-chip devices and microphysiological systems. *ACS Biomater Sci Eng* 7(7):2880–2899.  
<https://doi.org/10.1021/acsbomaterials.0c00640>
  58. Okhovatian S, Shakeri A, Davenport Huyer L et al (2023) Elastomeric polyesters in cardiovascular tissue engineering and organs-on-a-chip. *Biomacromolecules* 24(11):4511–4531.  
<https://doi.org/10.1021/acs.biomac.3c00387>
  59. Nguyen T, Jung SH, Lee MS et al (2019) Robust chemical bonding of PMMA microfluidic devices to porous PETE membranes for reliable cytotoxicity testing of drugs. *Lab Chip* 19(21):3706–3713.  
<https://doi.org/10.1039/c9lc00338j>
  60. Wnorowski A, Yang H, Wu JC (2019) Progress, obstacles, and limitations in the use of stem cells in organ-on-a-chip models. *Adv Drug Deliv Rev* 140:3–11.  
<https://doi.org/10.1016/j.addr.2018.06.001>
  61. Mano SS, Uto K, Ebara M (2020) Fluidity of poly ( $\epsilon$ -caprolactone)-based material induces epithelial-to-mesenchymal transition. *Int J Mol Sci* 21(5):E1757.  
<https://doi.org/10.3390/ijms21051757>
  62. Perrone E, Cesaria M, Zizzari A et al (2021) Potential of CO<sub>2</sub>-laser processing of quartz for fast prototyping of microfluidic reactors and templates for 3D cell assembly over large scale. *Mater Today Bio* 12:100163.  
<https://doi.org/10.1016/j.mtbio.2021.100163>
  63. Gold K, Gaharwar AK, Jain A (2019) Emerging trends in multi-scale modeling of vascular pathophysiology: organ-on-a-chip and 3D printing. *Biomaterials* 196:2–17.  
<https://doi.org/10.1016/j.biomaterials.2018.07.029>
  64. Hamid ISLA, Khim BK, Omar MFM et al (2022) Three-dimensional soft material micropatterning via grayscale photolithography for improved hydrophobicity of polydimethylsiloxane (PDMS). *Micromachines* 13(1):78.  
<https://doi.org/10.3390/mi13010078>
  65. Toepke MW, Kenis PJA (2005) Multilevel microfluidics via single-exposure photolithography. *J Am Chem Soc* 127(21):7674–7675.  
<https://doi.org/10.1021/ja050660+>
  66. Zhou S, Lu ZF, Yuan QX et al (2021) Measurement and compensation of a stitching error in a DMD-based step-stitching photolithography system. *Appl Opt* 60(29):9074–9081.  
<https://doi.org/10.1364/AO.434124>
  67. Sosa-Hernández JE, Villalba-Rodríguez AM, Romero-Castillo KD et al (2018) Organs-on-a-chip module: a review from the development and applications perspective. *Micromachines* 9(10):536.  
<https://doi.org/10.3390/mi9100536>
  68. Day JH, Nicholson TM, Su XJ et al (2020) Injection molded open microfluidic well plate inserts for user-friendly coculture and microscopy. *Lab Chip* 20(1):107–119.  
<https://doi.org/10.1039/c9lc00706g>
  69. Iliescu C, Taylor H, Avram M et al (2012) A practical guide for the fabrication of microfluidic devices using glass and silicon. *Biomicrofluidics* 6(1):016505.  
<https://doi.org/10.1063/1.3689939>
  70. Gharib G, Büttin İ, Munganlı Z et al (2022) Biomedical applications of microfluidic devices: a review. *Biosensors* 12(11):1023.  
<https://doi.org/10.3390/bios12111023>
  71. Włodarczyk KL, Carter RM, Jahanbakhsh A et al (2018) Rapid laser manufacturing of microfluidic devices from glass substrates. *Micromachines* 9(8):E409.  
<https://doi.org/10.3390/mi9080409>
  72. Zhou YF (2017) The recent development and applications of fluidic channels by 3D printing. *J Biomed Sci* 24(1):80.  
<https://doi.org/10.1186/s12929-017-0384-2>
  73. Kratz SRA, Höll G, Schuller P et al (2019) Latest trends in bio-sensing for microphysiological organs-on-a-chip and body-on-a-chip systems. *Biosensors* 9(3):110.  
<https://doi.org/10.3390/bios9030110>
  74. Bhatia SN, Ingber DE (2014) Microfluidic organs-on-chips. *Nat Biotechnol* 32(8):760–772.  
<https://doi.org/10.1038/nbt.2989>
  75. Liu J, Mosavati B, Oleinikov AV et al (2019) Biosensors for detection of human placental pathologies: a review of emerging technologies and current trends. *Transl Res* 213:23–49.  
<https://doi.org/10.1016/j.trsl.2019.05.002>
  76. Wang Q, Wang C, Yang XY et al (2023) Microfluidic preparation of optical sensors for biomedical applications. *Smart Med* 2(1):e20220027.  
<https://doi.org/10.1002/smmd.20220027>
  77. Fleming MR, Brown MR, Kronengold J et al (2016) Stimulation of slack K<sup>+</sup> channels alters mass at the plasma membrane by triggering dissociation of a phosphatase-regulatory complex. *Cell Rep* 16(9):2281–2288.  
<https://doi.org/10.1016/j.celrep.2016.07.024>
  78. Zirath H, Spitz S, Roth D et al (2021) Bridging the academic–industrial gap: application of an oxygen and pH sensor-integrated lab-on-a-chip in nanotoxicology. *Lab Chip* 21(21):4237–4248.  
<https://doi.org/10.1039/D1LC00528F>
  79. Wang XD, Wolfbeis OS (2014) Optical methods for sensing and imaging oxygen: materials, spectroscopies and applications. *Chem Soc Rev* 43(10):3666–3761.  
<https://doi.org/10.1039/C4CS00039K>
  80. Khalid MAU, Kim YS, Ali M et al (2020) A lung cancer-on-chip platform with integrated biosensors for physiological monitoring and toxicity assessment. *Biochem Eng J* 155:107469.  
<https://doi.org/10.1016/j.bej.2019.107469>
  81. Shaegh SAM, de Ferrari F, Zhang YS et al (2016) A microfluidic optical platform for real-time monitoring of pH and oxygen in microfluidic bioreactors and organ-on-chip devices. *Biomicrofluidics* 10(4):044111.  
<https://doi.org/10.1063/1.4955155>
  82. Shang YX, Chen ZY, Fu FF et al (2019) Cardiomyocyte-driven structural color actuation in anisotropic inverse opals. *ACS Nano* 13(1):796–802.  
<https://doi.org/10.1021/acsnano.8b08230>
  83. Zhu CZ, Yang GH, Li H et al (2015) Electrochemical sensors and biosensors based on nanomaterials and nanostructures. *Anal Chem* 87(1):230–249.  
<https://doi.org/10.1021/ac5039863>
  84. Maduraiveeran G, Sasidharan M, Ganesan V (2018) Electrochemical sensor and biosensor platforms based on advanced nanomaterials for biological and biomedical applications. *Biosens Bioelectron* 103:113–129.  
<https://doi.org/10.1016/j.bios.2017.12.031>
  85. Dornhof J, Kieninger J, Muralidharan H et al (2022) Microfluidic organ-on-chip system for multi-analyte monitoring of metabolites in 3D cell cultures. *Lab Chip* 22(2):225–239.  
<https://doi.org/10.1039/d1lc00689d>
  86. Du X, Zhang ZH, Zheng XD et al (2020) An electrochemical biosensor for the detection of epithelial-mesenchymal transition. *Nat Commun* 11:192.  
<https://doi.org/10.1038/s41467-019-14037-w>
  87. Odijk M, van der Meer AD, Levner D et al (2015) Measuring direct current trans-epithelial electrical resistance in organ-on-a-chip microsystems. *Lab Chip* 15(3):745–752.

- <https://doi.org/10.1039/C4LC01219D>
88. Henry OYF, Villenave R, Crounce MJ et al (2017) Organs-on-chips with integrated electrodes for trans-epithelial electrical resistance (TEER) measurements of human epithelial barrier function. *Lab Chip* 17(13):2264–2271. <https://doi.org/10.1039/c7lc00155j>
  89. Waithe OY, Peng X, Childs EW et al (2024) Measurement of trans-endothelial electrical resistance in blood-brain barrier endothelial cells. *Methods Mol Biol* 2711:199–203. [https://doi.org/10.1007/978-1-0716-3429-5\\_16](https://doi.org/10.1007/978-1-0716-3429-5_16)
  90. Shin W, Kim HJ (2022) 3D in vitro morphogenesis of human intestinal epithelium in a gut-on-a-chip or a hybrid chip with a cell culture insert. *Nat Protoc* 17(3):910–939. <https://doi.org/10.1038/s41596-021-00674-3>
  91. Lind JU, Busbee TA, Valentine AD et al (2017) Instrumented cardiac microphysiological devices via multimaterial three-dimensional printing. *Nat Mater* 16(3):303–308. <https://doi.org/10.1038/nmat4782>
  92. Qu KY, Cheng HY, Qiao L et al (2025) Construction of engineered cardiac tissue on a heart-on-a-chip device enables modeling of arrhythmogenic right ventricular cardiomyopathy. *Biosens Bioelectron* 281:117478. <https://doi.org/10.1016/j.bios.2025.117478>
  93. Bannerman D, Pascual-Gil S, Wu QH et al (2024) Heart-on-a-chip model of epicardial-myocardial interaction in ischemia reperfusion injury. *Adv Healthc Mater* 13(21):e2302642. <https://doi.org/10.1002/adhm.202302642>
  94. Yang JW, Khorsandi D, Trabucco L et al (2024) Liver-on-a-chip integrated with label-free optical biosensors for rapid and continuous monitoring of drug-induced toxicity. *Small* 20(48):2403560. <https://doi.org/10.1002/sml.202403560>
  95. Xie R, Korolj A, Liu C et al (2020) H-FIBER: microfluidic topographical hollow fiber for studies of glomerular filtration barrier. *ACS Cent Sci* 6(6):903–912. <https://doi.org/10.1021/acscentsci.9b01097>
  96. Wu J, Zhang B, Liu X et al (2024) An intelligent intestine-on-a-chip for rapid screening of probiotics with relief-enteritis function. *Adv Mater* 36(47):e2408485. <https://doi.org/10.1002/adma.202408485>
  97. Yang S, Zhang TY, Ge YL et al (2023) Sentinel supervised lung-on-a-chip: a new environmental toxicology platform for nanoplastic-induced lung injury. *J Hazard Mater* 458:131962. <https://doi.org/10.1016/j.jhazmat.2023.131962>
  98. Viegas J, Sarmiento B (2024) Bridging the gap between testing and clinics exploring alternative pre-clinical models in melanoma research. *Adv Drug Deliv Rev* 208:115295. <https://doi.org/10.1016/j.addr.2024.115295>
  99. Wang K, Man K, Liu J et al (2020) Microphysiological systems: design, fabrication, and applications. *ACS Biomater Sci Eng* 6(6):3231–3257. <https://doi.org/10.1021/acsbomaterials.9b01667>
  100. Lee Y, Kim MH, Alves DR et al (2021) Gut-kidney axis on chip for studying effects of antibiotics on risk of hemolytic uremic syndrome by Shiga toxin-producing *Escherichia coli*. *Toxins* 13(11):775. <https://doi.org/10.3390/toxins13110775>
  101. Ong LJY, Ching T, Chong LH et al (2019) Self-aligning TetrIS-Like (TILE) modular microfluidic platform for mimicking multi-organ interactions. *Lab Chip* 19(13):2178–2191. <https://doi.org/10.1039/C9LC00160C>
  102. Xu ZY, Li EC, Guo Z et al (2016) Design and construction of a multi-organ microfluidic chip mimicking the in vivo microenvironment of lung cancer metastasis. *ACS Appl Mater Interfaces* 8(39):25840–25847. <https://doi.org/10.1021/acsami.6b08746>
  103. Yang JD, Hirai Y, Iida K et al (2023) Integrated-gut-liver-on-a-chip platform as an in vitro human model of non-alcoholic fatty liver disease. *Commun Biol* 6:310. <https://doi.org/10.1038/s42003-023-04710-8>
  104. Zbinden A, Marzi J, Schlünder K et al (2020) Non-invasive marker-independent high content analysis of a microphysiological human pancreas-on-a-chip model. *Matrix Biol* 85:205–220. <https://doi.org/10.1016/j.matbio.2019.06.008>
  105. Shafagh RZ, Youhanna S, Keulen J et al (2022) Bioengineered pancreas-liver crosstalk in a microfluidic coculture chip identifies human metabolic response signatures in prediabetic hyperglycemia. *Adv Sci* 9(34):e2203368. <https://doi.org/10.1002/advs.202203368>
  106. Lei F, Liang MH, Liu Y et al (2021) Multi-compartment organ-on-a-chip based on electrospun nanofiber membrane as in vitro jaundice disease model. *Adv Fiber Mater* 3(6):383–393. <https://doi.org/10.1007/s42765-021-00091-x>
  107. Ren L, Liu WM, Wang YL et al (2013) Investigation of hypoxia-induced myocardial injury dynamics in a tissue interface mimicking microfluidic device. *Anal Chem* 85(1):235–244. <https://doi.org/10.1021/ac3025812>
  108. Rexus-Hall ML, Khalil NN, Escopete SS et al (2022) A myocardial infarct border-zone-on-a-chip demonstrates distinct regulation of cardiac tissue function by an oxygen gradient. *Sci Adv* 8(49):eabn7097. <https://doi.org/10.1126/sciadv.abn7097>
  109. Sung H, Ferlay J, Siegel RL et al (2021) Global cancer statistics 2020: GLOBOCAN estimates of incidence and mortality worldwide for 36 cancers in 185 countries. *CA A Cancer J Clin* 71(3):209–249. <https://doi.org/10.3322/caac.21660>
  110. Liu XX, Fang JR, Huang S et al (2021) Tumor-on-a-chip: from bioinspired design to biomedical application. *Microsyst Nanoeng* 7:50. <https://doi.org/10.1038/s41378-021-00277-8>
  111. Miller PG, Huang E, Fisher R et al (2025) Development of a microphysiological system to model human cancer metastasis from the colon to the liver. *Biotechnol Bioeng* 122(3):481–494. <https://doi.org/10.1002/bit.28890>
  112. Lee S, Kim YG, Jung HI et al (2024) Bone-on-a-chip simulating bone metastasis in osteoporosis. *Biofabrication* 16(4):045025. <https://doi.org/10.1088/1758-5090/ad6cf9>
  113. McCabe KM, Hsieh J, Thomas DG et al (2020) Antisense oligonucleotide treatment produces a type I interferon response that protects against diet-induced obesity. *Mol Metab* 34:146–156. <https://doi.org/10.1016/j.molmet.2020.01.010>
  114. Jiang H, Mao T, Liu Y et al (2022) Protective effects and mechanisms of Yinchen lingui zhugan decoction in HFD-induced nonalcoholic fatty liver disease rats based on network pharmacology and experimental verification. *Front Pharmacol* 13:908128. <https://doi.org/10.3389/fphar.2022.908128>
  115. Xu H, Chen GF, Ma YS et al (2020) Hepatic proteomic changes and Sirt1/AMPK signaling activation by oxymatrine treatment in rats with non-alcoholic steatosis. *Front Pharmacol* 11:216. <https://doi.org/10.3389/fphar.2020.00216>
  116. Wang BN, Wu CB, Chen ZM et al (2021) DL-3-n-butylphthalide ameliorates diabetes-associated cognitive decline by enhancing PI3K/Akt signaling and suppressing oxidative stress. *Acta Pharmacol Sin* 42(3):347–360. <https://doi.org/10.1038/s41401-020-00583-3>
  117. Maisels MJ, McDonagh AF (2008) Phototherapy for neonatal jaundice. *N Engl J Med* 358(9):920–928. <https://doi.org/10.1056/nejmct0708376>
  118. Yan J, Duan J, Wu X, et al (2015) Total saponins from *Aralia*

- taibaiensis protect against myocardial ischemia/reperfusion injury through AMPK pathway. *Int J Mol Med* 36 (6):1538–1546. <https://doi.org/10.3892/ijmm.2015.2391>
119. Trainor PJ, Yampolskiy RV, DeFilippis AP (2018) Wisdom of artificial crowds feature selection in untargeted metabolomics: an application to the development of a blood-based diagnostic test for thrombotic myocardial infarction. *J Biomed Inform* 81: 53–60. <https://doi.org/10.1016/j.jbi.2018.03.007>
  120. Poon MML, Farber DL (2020) The whole body as the system in systems immunology. *iScience* 23(9):101509. <https://doi.org/10.1016/j.isci.2020.101509>
  121. Grover P, Bhardwaj M, Mehta L et al (2022) Identification and characterization of in vitro metabolites of ibrutinib by rat liver microsomes using ultra-performance liquid chromatography coupled with tandem mass spectrometry. *Indian J Pharm Sci* 84(3):762–771. <https://doi.org/10.36468/pharmaceutical-sciences.971>
  122. Kang YBA, Rawat S, Cirillo J et al (2013) Layered long-term co-culture of hepatocytes and endothelial cells on a transwell membrane: toward engineering the liver sinusoid. *Biofabrication* 5(4):045008. <https://doi.org/10.1088/1758-5082/5/4/045008>
  123. Diehl AM, Chute J (2013) Underlying potential: cellular and molecular determinants of adult liver repair. *J Clin Invest* 123(5):1858–1860. <https://doi.org/10.1172/JCI69966>
  124. Lasser KE, Allen PD, Woolhandler SJ et al (2002) Timing of new black box warnings and withdrawals for prescription medications. *JAMA* 287(17):2215–2220. <https://doi.org/10.1001/jama.287.17.2215>
  125. Delalat B, Cozzi C, Ghaemi SR et al (2018) Microengineered bioartificial liver chip for drug toxicity screening. *Adv Funct Materials* 28(28):1801825. <https://doi.org/10.1002/adfm.201801825>
  126. Oleaga C, Riu A, Rothmund S et al (2018) Investigation of the effect of hepatic metabolism on off-target cardiotoxicity in a multi-organ human-on-a-chip system. *Biomaterials* 182:176–190. <https://doi.org/10.1016/j.biomaterials.2018.07.062>
  127. Yin F, Zhang X, Wang L et al (2021) HiPSC-derived multi-organoids-on-chip system for safety assessment of antidepressant drugs. *Lab Chip* 21(3):571–581. <https://doi.org/10.1039/d0lc00921k>
  128. Skardal A, Murphy SV, Devarasetty M et al (2017) Multi-tissue interactions in an integrated three-tissue organ-on-a-chip platform. *Sci Rep* 7:8837. <https://doi.org/10.1038/s41598-017-08879-x>
  129. Ronaldson-Bouchard K, Teles D, Yeager K et al (2022) A multi-organ chip with matured tissue niches linked by vascular flow. *Nat Biomed Eng* 6(4):351–371. <https://doi.org/10.1038/s41551-022-00882-6>
  130. Perazella MA (2009) Renal vulnerability to drug toxicity. *Clin J Am Soc Nephrol* 4(7):1275–1283. <https://doi.org/10.2215/cjn.02050309>
  131. Zhang C, Peng F, Liu W et al (2014) Nanostructured lipid carriers as a novel oral delivery system for triptolide: induced changes in pharmacokinetics profile associated with reduced toxicity in male rats. *Int J Nanomed* 9:1049–1063. <https://doi.org/10.2147/IJN.S55144>
  132. Li ZY, Jiang L, Zhu YJ et al (2018) Assessment of hepatic metabolism-dependent nephrotoxicity on an organs-on-a-chip microdevice. *Toxicol Vitro* 46:1–8. <https://doi.org/10.1016/j.tiv.2017.10.005>
  133. Theobald J, Ghanem A, Wallisch P et al (2018) Liver-kidney-on-chip to study toxicity of drug metabolites. *ACS Biomater Sci Eng* 4(1):78–89. <https://doi.org/10.1021/acsbiomaterials.7b00417>
  134. Huang QH, Yang TH, Song YP et al (2024) A three-dimensional (3D) liver–kidney on a chip with a biomimicking circulating system for drug safety evaluation. *Lab Chip* 24(6): 1715–1726. <https://doi.org/10.1039/D3LC00980G>
  135. de Gregorio V, Telesco M, Corrado B et al (2020) Intestine–liver axis on-chip reveals the intestinal protective role on hepatic damage by emulating ethanol first-pass metabolism. *Front Bioeng Biotechnol* 8:163. <https://doi.org/10.3389/fbioe.2020.00163>
  136. Lee DW, Ha SK, Choi I et al (2017) 3D gut–liver chip with a PK model for prediction of first-pass metabolism. *Biomed Microdevices* 19(4):100. <https://doi.org/10.1007/s10544-017-0242-8>
  137. Trapecar M, Communal C, Velazquez J et al (2020) Gut–liver physiometrics reveal paradoxical modulation of IBD-related inflammation by short-chain fatty acids. *Cell Syst* 10(3): 223–239.e9. <https://doi.org/10.1016/j.cels.2020.02.008>
  138. Chen WLK, Edington C, Suter E et al (2017) Integrated gut/liver microphysiological systems elucidates inflammatory inter-tissue crosstalk. *Biotechnol Bioeng* 114(11):2648–2659. <https://doi.org/10.1002/bit.26370>
  139. Lucchetti M, Aina KO, Grandmougin L et al (2024) An organ-on-chip platform for simulating drug metabolism along the gut–liver axis. *Adv Healthc Mater* 13(20):e2303943. <https://doi.org/10.1002/adhm.202303943>
  140. Iori E, Vinci B, Murphy E et al (2012) Glucose and fatty acid metabolism in a 3 tissue in-vitro model challenged with normo- and hyperglycaemia. *PLoS ONE* 7(4):e34704. <https://doi.org/10.1371/journal.pone.0034704>
  141. Zhang C, Zhao ZQ, Abdul Rahim NA et al (2009) Towards a human-on-chip: culturing multiple cell types on a chip with compartmentalized microenvironments. *Lab Chip* 9(22):3185–3192. <https://doi.org/10.1039/B915147H>
  142. Oleaga C, Bernabini C, Smith AS et al (2016) Multi-organ toxicity demonstration in a functional human in vitro system composed of four organs. *Sci Rep* 6:20030. <https://doi.org/10.1038/srep20030>
  143. Nigam AK, Ojha AA, Li JG et al (2021) Molecular properties of drugs handled by kidney OATs and liver OATPs revealed by chemoinformatics and machine learning: implications for kidney and liver disease. *Pharmaceutics* 13(10):1720. <https://doi.org/10.3390/pharmaceutics13101720>
  144. Maschmeyer I, Lorenz AK, Schimek K et al (2015) A four-organ-chip for interconnected long-term co-culture of human intestine, liver, skin and kidney equivalents. *Lab Chip* 15(12): 2688–2699. <https://doi.org/10.1039/c5lc00392j>
  145. Rajan SAP, Aleman J, Wan MM et al (2020) Probing prodrug metabolism and reciprocal toxicity with an integrated and humanized multi-tissue organ-on-a-chip platform. *Acta Biomater* 106:124–135. <https://doi.org/10.1016/j.actbio.2020.02.015>
  146. Wang X, Cirit M, Wishnok JS et al (2019) Analysis of an integrated human multiorgan microphysiological system for combined tolcapone metabolism and brain metabolomics. *Anal Chem* 91(13):8667–8675. <https://doi.org/10.1021/acs.analchem.9b02224>
  147. Edington CD, Chen WLK, Geishecker E et al (2018) Interconnected microphysiological systems for quantitative biology and pharmacology studies. *Sci Rep* 8:4530. <https://doi.org/10.1038/s41598-018-22749-0>

148. Miller PG, Shuler ML (2016) Design and demonstration of a pumpless 14 compartment microphysiological system. *Biotechnol Bioeng* 113(10):2213–2227. <https://doi.org/10.1002/bit.25989>
149. Adler M, Ramm S, Hafner M et al (2016) A quantitative approach to screen for nephrotoxic compounds in vitro. *J Am Soc Nephrol* 27(4):1015–1028. <https://doi.org/10.1681/asn.2015010060>
150. Yoon S, You DK, Jeong U et al (2024) Microfluidics in high-throughput drug screening: organ-on-a-chip and *C. elegans*-based innovations. *Biosensors* 14(1):55. <https://doi.org/10.3390/bios14010055>
151. Wang YY, Gu TX, Tian XL et al (2021) A small molecule antagonist of PD-1/PD-L1 interactions acts as an immune checkpoint inhibitor for NSCLC and melanoma immunotherapy. *Front Immunol* 12:654463. <https://doi.org/10.3389/fimmu.2021.654463>
152. van der Zanden SY, Luimstra JJ, Neefjes J et al (2020) Opportunities for small molecules in cancer immunotherapy. *Trends Immunol* 41(6):493–511. <https://doi.org/10.1016/j.it.2020.04.004>
153. Cecen B, Karavasili C, Nazir M et al (2021) Multi-organs-on-chips for testing small-molecule drugs: challenges and perspectives. *Pharmaceutics* 13(10):1657. <https://doi.org/10.3390/pharmaceutics13101657>
154. Gribkoff VK, Kaczmarek LK (2017) The need for new approaches in CNS drug discovery: why drugs have failed, and what can be done to improve outcomes. *Neuropharmacology* 120:11–19. <https://doi.org/10.1016/j.neuropharm.2016.03.021>
155. Fridén M, Winiwarter S, Jerndal G et al (2009) Structure-brain exposure relationships in rat and human using a novel data set of unbound drug concentrations in brain interstitial and cerebrospinal fluids. *J Med Chem* 52(20):6233–6243. <https://doi.org/10.1021/jm901036q>
156. Peng B, Tong ZQ, Tong WY et al (2020) In situ surface modification of microfluidic blood–brain-barriers for improved screening of small molecules and nanoparticles. *ACS Appl Mater Interfaces* 12(51):56753–56766. <https://doi.org/10.1021/acscami.0c17102>
157. Shoemaker RH (2006) The NCI60 human tumour cell line anti-cancer drug screen. *Nat Rev Cancer* 6(10):813–823. <https://doi.org/10.1038/nrc1951>
158. Pampaloni F, Reynaud EG, Stelzer EHK (2007) The third dimension bridges the gap between cell culture and live tissue. *Nat Rev Mol Cell Biol* 8(10):839–845. <https://doi.org/10.1038/nrm2236>
159. Lee J, Cuddihy MJ, Kotov NA (2008) Three-dimensional cell culture matrices: state of the art. *Tissue Eng Part B Rev* 14(1):61–86. <https://doi.org/10.1089/teb.2007.0150>
160. Zhu YX, Jiang DM, Qiu Y et al (2024) Dynamic microphysiological system chip platform for high-throughput, customizable, and multi-dimensional drug screening. *Bioact Mater* 39:59–73. <https://doi.org/10.1016/j.bioactmat.2024.05.019>
161. Lee DW, Choi YS, Seo YJ et al (2014) High-throughput screening (HTS) of anticancer drug efficacy on a micropillar/microwell chip platform. *Anal Chem* 86(1):535–542. <https://doi.org/10.1021/ac402546b>
162. Huh D, Fujioka H, Tung YC et al (2007) Acoustically detectable cellular-level lung injury induced by fluid mechanical stresses in microfluidic airway systems. *Proc Natl Acad Sci USA* 104(48):18886–18891. <https://doi.org/10.1073/pnas.0610868104>
163. Huang Y, Liu T, Huang Q et al (2024) From organ-on-a-chip to human-on-a-chip: a review of research progress and latest applications. *ACS Sens* 9(7):3466–3488. <https://doi.org/10.1021/acssensors.4c00004>
164. Herland A, Maoz BM, Das D et al (2020) Quantitative prediction of human pharmacokinetic responses to drugs via fluidically coupled vascularized organ chips. *Nat Biomed Eng* 4(4):421–436. <https://doi.org/10.1038/s41551-019-0498-9>
165. Trapecar M, Wogram E, Svoboda D et al (2021) Human physiologic model integrating microphysiological systems of the gut, liver, and brain for studies of neurodegenerative diseases. *Sci Adv* 7(5):eabd1707. <https://doi.org/10.1126/sciadv.abd1707>
166. Dave R, Pandey K, Patel R et al (2025) Leveraging 3D cell culture and AI technologies for next-generation drug discovery. *Cell Biomater* 1(3):100050. <https://doi.org/10.1016/j.celbio.2025.100050>
167. Oikonomou EK, Khara R (2023) Machine learning in precision diabetes care and cardiovascular risk prediction. *Cardiovasc Diabetol* 22(1):259. <https://doi.org/10.1186/s12933-023-01985-3>
168. Schuhmacher A, Brieke C, Gassmann O et al (2021) Systematic risk identification and assessment using a new risk map in pharmaceutical R&D. *Drug Discov Today* 26(12):2786–2793. <https://doi.org/10.1016/j.drudis.2021.06.015>
169. Ghebrehiwet I, Zaki N, Damseh R et al (2024) Revolutionizing personalized medicine with generative AI: a systematic review. *Artif Intell Rev* 57(5):128. <https://doi.org/10.1007/s10462-024-10768-5>
170. Chia BS, Seah YFS, Wang B et al (2025) Engineering a new generation of gene editors: integrating synthetic biology and AI innovations. *ACS Synth Biol* 14(3):636–647. <https://doi.org/10.1021/acssynbio.4c00686>
171. Wessels HH, Stirn A, Méndez-Mancilla A et al (2024) Prediction of on-target and off-target activity of CRISPR–Cas13d guide RNAs using deep learning. *Nat Biotechnol* 42(4):628–637. <https://doi.org/10.1038/s41587-023-01830-8>
172. Jeong SH, Lee HJ, Lee SJ (2023) Recent advances in CRISPR–Cas technologies for synthetic biology. *J Microbiol* 61(1):13–36. <https://doi.org/10.1007/s12275-022-00005-5>